

BIOACTIVE MOLECULES FROM HALOTOLERANT YEAST

A Dissertation for

Course code and Course Title: GBT-651 and Dissertation

Credits: 16

Submitted in partial fulfilment of the requirements for the degree of
Master of Science in Biotechnology

by

Ms. MELISHA CARDOSO

Seat number: 22PO470009

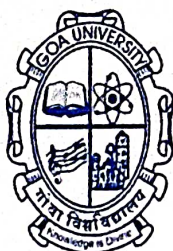
ABC ID: 843-285-940-086

PRN: 201900335

Under the Supervision of

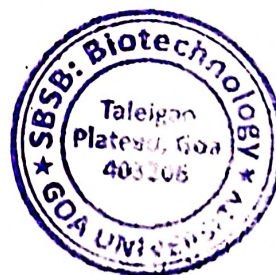
Mrs. DVITI LAVESH VOLVOIKAR

School of Biological Sciences and Biotechnology



Goa University

8th April 2024



Seal of the School

Examined by

D. P. Dapari

S. B. S. B.
8/4/24

Qy

M. V. M. V.

M. V. M. V.
8/4/2024

M. V. M. V.
8/4/24

M. V. M. V.

DECLARATION BY STUDENT

I hereby declare that the data presented in this Dissertation report entitled, "Bioactive molecules from Halotolerant yeast" is based on the results of investigations carried out by me in the at the school of biological sciences and Biotechnology, Goa University under the Supervision of Mrs Dviti L. Volvoikar and the same has not been submitted elsewhere for the award of a degree or diploma by me. Further, I understand that Goa University or its authorities / College will be not be responsible for the correctness of observations / experimental or other findings given the dissertation.

I hereby authorize the University/college authorities to upload this dissertation on the dissertation repository or anywhere else as the UGC regulations demand and make it available to any one as needed.



Signature and Name of Student: Melisha Cardoso

Seat no: 22PO470009

Date: 8/4/24

Place: Goa University

COMPLETION CERTIFICATE

This is to certify that the dissertation report “**Bioactive molecules from Halotolerant yeast**” is a bonafide work carried out by **Ms. Melisha Cardoso** under my supervision in partial fulfilment of the requirements for the award of the degree of **Master Of Science In Biotechnology** in the Discipline of Biotechnology at the School of biological sciences and Biotechnology, Goa University.

Dviti

Mrs Dviti L. Volvoikar

Date: 08/04/2024



[Signature]
Signature of Dean of the School

School/Dept Stamp

Date: 8/4/24

Place: Goa University

**Dean of School of Biological Sciences
& Biotechnology
Goa University, Goa-403206**

CONTENTS

Chapter	Particulars	Page numbers
	Preface	i
	Acknowledgments	ii
	Tables and Figures	v
	Abbreviations used	vii
	Abstract	xi
1	Introduction	1
	1.1 Background	2
	1.2 Aim and Objectives	8
	1.3 Hypothesis	9
	1.4 Scope	9
2	Literature Review	10
3	Methodology	17
4	Analysis and Conclusions	31
	References	78
	Appendix I: media	83
	Appendix II: reagents	90

PREFACE

In the realm of Biotechnology, the exploration of extremophiles has garnered substantial interest due to their remarkable adaptability to extreme environmental conditions. Among these extremophiles, halophilic yeast species have emerged as compelling candidates for bioprospecting endeavors. This preface sets the stage for a comprehensive investigation into the bioactive molecules derived from a halotolerant yeast strain, designated SPDM15.

Halophilic organisms, thrive in high-salt environments, possessing unique biochemical pathways tailored to endure osmotic stressors. The strain SPDM15, characterized by its robustness across a spectrum of salinities, presents an intriguing model system for probing the biosynthesis of bioactive compounds. Pigments and enzymes are noteworthy among its repertoire of metabolic products, whose potential applications span diverse industrial sectors. The various characteristics of SPDM15 make it an interesting subject to study in order to find better ways to implement sustainable waste management practices. This yeast strain shows potential for speeding up composting with its enzymes, offering a way to deal with the increasing problem of organic waste. Additionally, the pigments synthesized by SPDM15 present opportunities for novel applications, including environmentally friendly dyeing processes.

This project seeks to understand which bioactive molecules SPDM15 produces and its potential application in biotechnology.

ACKNOWLEDGEMENT

I would like to express my sincere gratitude to my guide, Mrs. Dviti L. Volvoikar, for her valuable suggestions and advice and for helping me throughout my research.

I would like to express my gratitude to Dean Bernard F. Rodrigues, Vice Dean Professor Sanjeev Ghadi, Dr Samantha Fernandes, Ms Snesha Bhomkar and especially programme Director Dr Megnath Prabhu of the School of Biological Sciences and Biotechnology for his valuable guidance and advice.

I'm also extremely thankful to Vice Dean Sunder N. Dhuri, research scholar Disha Gauns for providing CHNS analysis data, Mr Prajot Chari for FTIR analysis data and Prof Prajesh S. Volvoikar for allowing me to use the Rotary evaporator from the School of Chemical Sciences.

I would like to take this opportunity to express my appreciation to the research scholars especially Ms Hetika Kotecha for all the help and advice; laboratory staff, namely Mr. Ashish, Mr. Serrao, Mr. Sameer, Mrs Sanjana, Mrs Jaya and Mrs Sandhya, for providing the necessary requirements, managing work, and most importantly, for their unwavering support and encouragement.

A special thanks to my friends, especially Mark Rodrigues and all my classmates, for their support and timely help throughout my dissertation work.

Lastly, I also extend a big thank you to my parents, Mr. Caetano Cardoso and Mrs. Damiana Fernandes, for their supportive environment and encouragement.

TABLES

Table No.	Description	Page no.
1	Different types of mordants for post and pre mordanting of cotton fabric	22
2	Composting process with different sets containing different raw material.	28
3	Growth Studies of SPDM15 at various salt concentrations.	32
4	Absorbance at 10% salt concentration on different days .	34
5	pH analysis of compost	59
6	Analysis of compost of day 1 for various parameters such as moisture, TS, Ash, VS for all the different sets of compost .	61
7	Monitoring of temperature for all sets for 20 days	64
8	Determination of germination rate (%) and Vigor index to estimate the phytotoxicity of compost.	71
9	Analysis of compost for CHNS content to determine the maturity of compost.	73

FIGURES

Figure No.	Description	Page no.
1	The growth studies of isolate SPDM15 at various salt concentrations.	33
2	Isolate SPDM15 absorbance measured at 600 nm.	34
3	SEM analysis of isolate SPDM15 grown in NTYE broth at 10% salt concentration.	35
4	Morphology of isolate SPDM15 grown in NTYE broth at different salt concentrations.	38
5	Yeast viability (colony forming unit per ml) on 10% NTYE media	39
6	Significant alignments of isolate SPDM15 showing maximum identity with <i>Hortaea werneckii</i> species	43
7	Phylogenetic tree of SPDM15 species and related taxa, based on the ITS region	44
8	Hemolysis test to check the pathogenicity of isolate SPDM15	45
9	Pigment extracted from SPDM15 after growing in 10% NTYE media.	46
10	Infra-red spectrum (FT-IR) of melanin pigment of SPDM15 at 10% salt concentration	48
11	Standard FTIR spectra of melanin(Kiran et al., 2015)	48
12	Textile dyeing using melanin pigment extracted from the isolate SPDM15	50
13	Antibacterial property of dyed cloth with mordant Alum + Sodium carbonate	53

14	Extracellular enzyme production test. a). b) xylanase. c) pectinase. d) cellulase. e) amylase. f) gelatinase. g) urease. h) catalase. i) esterase. j) laccase. k) agarase. l) lipase m) Chitinase	55
15	Yeast isolate screened for EPS production	57
16	Screening of biosurfactants by CTAB-methylene blue agar test	58
17	pH analysis of compost on day 0, 10 and 25	60
18	Compost analysed for various parameters such as pH, moisture, TS, VS, Ash.	62
19	Temperature monitored for 25 days of different compost sets	65
20	Compost on 25th day	67
21	Phytotoxicity analysis using Cowpea (<i>Vigna unguiculata</i>) seeds against various sets of day 0	68
22	Germination rate determination using Cowpea (<i>Vigna unguiculata</i>) seeds against various sets at day 3	69
23	CHNS analysis of 25 th day compost sets.	74
24	C:N ratio of 25 th day compost sets.	74

ABBREVIATIONS USED

Entity	Abbreviation
Percentage	%
Degree of Celsius	°C
Milligrams	mg
Grams	g
Micrograms	µg
Microlitres	µl
Millilitres	ml
Nanometer	nm
Litres	L
Pounds per square inch	Psi
Volume	Vol
Scanning Electron Microscopy	SEM
Revolutions per minute	Rpm
Distilled water	DW
Hydrogen ion concentration	pH
milligrams per litre	mg/L
milligrams per millilitre	mg/ml
Species	Sp.
Seconds	Sec
minutes	min
Room Temperature	RT

Concentration	Conc.
hours	hrs
Mueller Hinton's Agar	MHA
Nacl Tryptone Yeast Extract	NTYE
Not Detected	ND

ABSTRACT

The current study investigated the characteristics and potential applications of Halotolerant yeast isolate SPDM15 in various biotechnological processes. The influence of salt concentration on yeast growth and morphology was explored, revealing significant variations in growth rates and structural changes in response to different salt levels. Notably, robust growth and proliferation were observed when grown in NTYE with 10% salt concentration, with distinct morphological alterations observed at varying concentrations. The pigment was soluble in DMSO and NaOH and was confirmed to be melanin through FTIR analysis. The dyeing experiment showcased the importance of mordant selection in achieving optimal dye absorption. Cotton fabric treated with Alum + Sodium carbonate and Alum + Ferrous sulphate exhibited superior pigment absorption and binding properties, with minimal colour fading observed after washing, wet rubbing and exposure to sunlight. Additionally, the antimicrobial activity of cotton fabric dyed with melanin pigment and treated with specific mordants highlighted the potential for antimicrobial textile applications. Further analysis unveiled the enzymatic activities of SPDM15, showcasing a diverse range of enzymes. Due to plant polymers' degradation ability, the isolate was employed for the compost accelerating process. The composting experiment demonstrated that compost T3 showed good maturity with a C: N ratio of 11.43 in 25 days.

Keywords: Salt crystal · *Hortaea* sp. Strain · SPDM15 · Halotolerant · Compost. Dyeing.

CHAPTER 1

INTRODUCTION

1. 1 Background

For a prolonged period, scientists have mainly focused on studying prokaryotic organisms like bacteria in very harsh places. This has made research mainly about bacteria. Solar salterns, characterized by high concentrations of sodium chloride (NaCl), other ions, UV irradiation, and occasionally extreme pH, were initially presumed to harbour prokaryotes solely. However, fungi were identified as active inhabitants of solar salterns. Subsequently, numerous novel species, including those previously recognized solely as contaminants in food, have been uncovered in hypersaline environments across the globe (Gunde-Cimerman et al., 2009)

1.1.1 *Hortaeawerneckii*, a halotolerant black yeast

Hortaea werneckii, a halophilic black yeast belonging to the *Teratosphaeriaceae* family within the *Capnodiales* order, is renowned as one of the extensively studied black yeasts and serves as a model organism for understanding halotolerant mechanisms in Eukarya (Rizk & Magdy, 2022). These black yeasts, known as polymorphic fungi, exhibit various growth forms, including yeast-like, filamentous, and meristematic growth, with hyphal growth predominantly observed on solidified media (Elsayis et al., 2022).

Eco physiological and morphological studies conducted under saline conditions in vitro have revealed the complex polymorphic life cycle of *H. werneckii*. This life cycle comprises hydrophilic yeast cells, hydrophobic hyphae, and meristematic growth, which appear well-suited for survival in the dynamic extreme environment of salterns. Until 2000, *H. werneckii* was mainly known as the cause of a skin condition called tinea nigra. This condition is a surface infection of the hands and feet that can happen in warmer areas. (de Hoog et al. 2000, Perez et al. 2005, Bonifaz et al. 2008). Infections typically occur when the skin is damaged and exposed to very salty water, especially in combination with excessive sweating. There

have also been cases linked to animal bites. However, it was unclear whether *H. werneckii* could cause more serious infections because it was thought that it couldn't grow at human body temperature (37°C). (de Hoog et al. 2000, Ng et al. 2005).

Studies on its adaptations have elucidated novel mechanisms enabling *H. werneckii* to thrive in highly saline environments and rapidly adapt to varying salt concentrations. These adaptations and their polymorphic life cycle confer dominance among fungi inhabiting hypersaline waters in eutrophic salterns. Variations in cell-wall pigmentation and structure, membrane fluidity, and compatible solutes have been observed, suggesting the presence of dual sets of genes involved in adaptation to hypersaline environments (Gunde-Cimerman & Plemenitaš, 2006b).

In halotolerant and halophilic fungi, polyols such as glycerol, erythritol, inositol, arabinitol, xylitol, and mannitol serve as prevalent compatible solutes. The High osmolarity glycerol (HOG) pathway plays a crucial role in the adaptation mechanisms of halophilic *H. werneckii* (Plemenitaš & Gunde-Cimerman, 2005b). Within this pathway, two important kinases (HwHog1A and HwHog1B) function as sensors, detecting elevated salt concentrations in the environment. These kinases become activated when the salinity exceeds 3.0 M NaCl, then they migrate to the nucleus where they trigger the expression of genes that aid in protecting the microorganism from the extreme conditions. Researchers discovered that when they inhibited the activity of these kinases using a compound called BPTIP, the growth of *H. werneckii* was impaired or halted entirely. Additionally, melanin, a pigment, may also play a role in the growth and maintenance of *H. werneckii's* cell wall. This was evident as a lack of melanin resulted in observable changes in the fungus's size and shape (Kejžar et al., 2015)

Glycerol is the primary compatible solute in *H. werneckii*, with quantities of other solutes varying based on the salinity of the growth medium and growth phase of the fungal culture.

However, the overall number of polyols, primarily glycerol, correlates positively with increasing salinity across all growth phases (Plemenitaš et al., 2008b).

1.1.2 Significance of melanin pigment.

Melanin pigments represent a class of high molecular weight metabolites characterized by negative charge and hydrophobic properties, displaying a colour spectrum ranging from brown to black. These pigments are synthesized from phenolic or indolic compounds and are commonly associated with proteins or carbohydrates in complex formations. The fundamental processes underlying melanin formation can be attributed to either the auto-oxidation of phenolic compounds within the medium or enzymatic pathways facilitated by key enzymes, specifically tyrosinase and polyketide synthase, playing pivotal roles in melanogenesis. (Elsayis et al., 2022)

Various types of melanin, such as eumelanins, phaeomelanins, allomelanins, and pyromelanins, have been identified in bacteria, fungi, and animals. Fungal melanins, a complex group of pigments, are synthesized through two distinct pathways: the DHN (1,8-dihydroxynaphthalene) and L-DOPA (L-3,4-dihydroxyphenyl-alanine) pathways, dependent on the fungal species (Helan et al., 2013). Generally, fungal DOPA-melanins originate from the oxidation of L-dopa or L-tyrosine, while DHN-melanins, characterized by the absence of nitrogen, represent another major fungal melanin type (Elsayis et al., 2022).

In the UV absorption spectrum, melanin demonstrates absorption peaks ranging from 235 nm to 300 nm (Helan et al., 2013). The melanization of the cell wall serves as a protective mechanism, aiding in preventing water loss, intracellular compatible solute leakage, and maintaining membrane fluidity. This adaptive feature enables fungi to thrive in environments with elevated salinity levels. The composition and structure of the melanin layer are influenced by the concentration of salt; under higher salinity conditions, the cell wall

becomes more porous, resulting in the release of glycerol and an increase in its extracellular levels. Conversely, at lower sodium chloride concentrations, melanin granules form a thin, continuous layer on the outer surface of the cell wall. (Śliżewska et al., 2022).

Notably, melanin exhibits significant antioxidant activity, scavenging free radicals across various scales. This property has been demonstrated to protect microorganisms from UV radiation, microbial lysis, oxidative stress induced by alveolar macrophages, and host plant and animal defence responses against fungal infections (Elsayis et al., 2022b).

Commercially, melanin finds application as a constituent in photoprotective creams designed for anti-melanoma therapy. Additionally, it has been reported to exhibit immunopharmacological properties. Recent investigations have revealed melanin's pronounced immunogenicity and anti-inflammatory attributes (Helan et al., 2013). Evaluating the cytotoxicity of melanin's derived from *H. werneckii* AS1 towards mammalian cells is imperative for medical and pharmaceutical purposes. Notably, the melanin from *H. werneckii* AS1 has demonstrated non-cytotoxic characteristics, displaying an IC50 exceeding 100 g/ml (Elsayis et al., 2022b).

1.1.3 Dyeing of cloth with melanin pigment extracted from black yeast.

Using non-allergenic, non-toxic, and environmentally friendly natural dyes in textile industries has gained significant attraction due to heightened environmental consciousness, aiming to circumvent hazardous synthetic dyes (Agarwal et al., 2009). The market potential of natural dyes is anticipated to surge in both large and small-scale sectors.

Derived from various plant and animal sources such as *Hibiscus mutabilis*, *Kema lacca*, grape pomace, Eucalyptus, tea, and vegetables, natural dyes find application in dyeing a range of textile materials including cotton, jute, wool, synthetic fibers, and silk (Freitas et al.,

2014). However, the drawback of natural dyes lies in their extraction yield factors, resulting in a relatively high market price of about US \$1/g, thereby limiting their usage to premium natural-coloured garments. To overcome this limitation, exploring alternative biological sources like fungi, bacteria, and algae for natural pigment production has been recommended, with recent studies highlighting the potential of fungal pigments in textile dyeing (Velmurugan et al., 2010).

Fungal dyes and pigments, sourced from diverse fungal species, offer significant potential across pharmaceuticals, food, cosmetics, and textiles, owing to their inherent biological functions such as resistance and protection against environmental stressors (Eisenman et al., 2012). The rising ecological consciousness among consumers favors the utilization of natural products, with the biodegradable and sustainable nature of fungal dyes and pigments presenting distinct advantages over synthetic counterparts (Shahid et al., 2013). However, challenges persist, including irregular fixation of some compounds even with mordants and the absence of standardized industrial dyeing methods tailored for these substances, necessitating the development of appropriate industrial-scale dyeing techniques (Weber et al., 2014). Consequently, refining and adapting dyeing methodologies to industrial conditions emerge as crucial steps to facilitate the widespread adoption of fungal dyes and pigments in textile applications.

1.1.4 Composting

Composting is one of the most efficient and efficacious treatment methods that can be employed for the removal of organic fractions of solid waste. It is an economically feasible and environmentally sustainable technique that can be used for the effective treatment of solid waste around the world. The main purpose of composting is to convert solid organic

wastes into nutrient-rich soil conditioners and organic fertilizer, which results in a reduction of odor, phytotoxic chemicals, weed seeds, and pathogens (Mahapatra et al., 2022).

It is an aerobic-microbial process of breaking organic matter (OM) into usable substances. It is basically a combination of mesophilic and thermophilic stages that finally results in the conversion of organic waste into a stable agronomic value product (Samal et al., 2018)

For a nutrient-rich compost, the organic waste should mainly consist of kitchen waste, also known as green waste (like fruits and vegetable leftovers, bread, cardboard, etc.), and garden waste, also known as brown waste (like fallen leaves, small wood chips, sawdust, plant leftovers, etc.). Combining these green and brown wastes helps maintain the carbon-to-nitrogen (C/N) ratio (Jouhara et al., 2017). The general recommended value of the (total) C/N ratio in substrates is between 25 and 30 (Haug, 1993). Epstein (2011) indicates that at a ratio of $C/N > 30$, the rate of decomposition is slow because of the little N available for microorganisms, while at $C/N < 20$, the excess of N is released in the form of NH_3 , resulting in losses of nutrients and generating potential malodors.

The process of composting can be bifurcated into three underlying phases. In the first phase, the OM is mixed with dry bulking agents like cow dung, curd, shredded paper, rice hulls, etc., which help provide adequate space for the disintegration of the OM with the assistance of microorganisms. In mesophilic conditions (moderate temperature), microorganisms with natural ventilation break down the OM into smaller particles. These particles hold more surface area, so the degradation process increases in the second phase. Mixing of particles needs to be done in regular intervals as a low aeration rate will prevent evaporation of moisture, which will tend to decrease the rate of decomposition. Microorganisms help maintain a porous structure of compost, which further helps distribute water and nutrients. Compost stays in this condition for several days to about a month. Excess water (called

leachate) is generated in the process of composting, which is highly rich in nutrients. Leachate from compost is generally yellowish-dark brown in colour. Dissolved and particulate OM in the composting leachate are essential sources of C, H, N, O, and P. Nitrogen and OM are generally considered the two main contaminants in composting leachate (Azim et al., 2018).

Aerobic composting under thermophilic conditions may be a widely practiced methodology for the decomposition of organic wastes. Though the optimum temperature for composting is 60°C, sometimes the temperature may rise to over 60°C throughout. This temperature variation may depend on the type, and quantity of the material used, climatic conditions prevailing around, and the size of the pile adopted (Tang et al., 2004)

1.2 Aim and objectives

Aim: -To screen for various bioactive molecules from halotolerant yeast.

Objectives

- Morphological and Physiological studies of Halotolerant yeast SPDM15.
- Screening and partial characterization of bioactive molecules produced by Halotolerant yeast.
- Evaluating the potential application of bioactive molecules produced by Halotolerant yeast.

1.3 Hypothesis / Research Question

The hypotheses for this study encompass several key aspects. Firstly, it is hypothesized that the microorganism thrives best at a 10% salt concentration. Secondly, that culture is non-pathogenic. Thirdly, it is proposed that the isolate SPDM15 secretes numerous plant polymer degrading enzymes so it can be capable of accelerating the composting process. Lastly, it is suggested that the microorganism has the ability to produce melanin pigment, which is known for its antibacterial properties and could potentially be utilized in fabric dyeing applications.

1.3 Scope

The application potential of SPDM15 spans various domains. firstly, it can aid in wastewater treatment due to the production of a diverse range of enzymes and extracellular polymeric substances (EPS), which could aid in heavy metal absorption. Additionally, compatible solutes from SPDM15 can be extracted. The pigment synthesized by the yeast can have potential applications in the cosmetics industry, such as nail polish, with potential antibacterial properties. Furthermore, research efforts can be directed toward investigating the antioxidant properties of melanin pigment, with implications for innovative medical and industrial applications. Lastly, the study can aim to elucidate the role of membrane lipids in aiding yeast survival in highly saline environments, potentially informing biotechnological strategies for environments with elevated salt concentrations.

CHAPTER 2

LITERATURE

REVIEW

2.1 Ecology of *Hortaea werneckii*

Hortaea werneckii, identified as a highly halotolerant fungus within the black yeast group, has been isolated from diverse marine environments (Elsayed et al., 2016). It is commonly found in thalasso-haline brines within salterns across multiple continents, spanning temperate, subtropical, and tropical climates, excluding subpolar and polar regions. The fungus primarily thrives in eutrophic thalasso-haline waters at moderate temperatures and is notably absent in oligotrophic or athalasso-haline hypersaline waters. Occasional occurrences have been reported in hypersaline waters with elevated temperatures. *Hortaeawerneckii* has been identified in seawater, on rocks near seawater, and in various marine habitats, including sea sponges, corals, marine fish, salted freshwater fish, beach soil, saltern microbial mats, salt marsh plants, and as an endophyte in mangrove plants (Zalar et al., 2019).

However, the survival of *H. werneckii* appears to be limited to eutrophic thalasso-haline waters in salterns within temperate climatic zones. Instances of its retrieval are sporadic, such as in salterns in Puerto Rico, but it has never been identified in oligotrophic salterns in Eilat at the Red Sea in Israel or in athalassohaline waters of the Dead Sea or Salt Lake, Utah (Gunde-Cimerman & Plemenitaš, 2006).

2.2 Plant polymer degrading enzymes production by halotolerant yeast.

As per research findings, four strains of *Hortaea werneckii* originating from Brazil demonstrated the ability to produce enzymes such as amylase, lipase, esterase, pectinase, and/or cellulase. These enzymes are known to target components within plant cells as their substrates. Notably, the strains did not exhibit expression of albuminase, keratinase, phospholipase, and DNase, which typically target substances associated with animals. Urease production was consistently positive across all isolates, while caseinase, gelatinase, and laccase production varied among the different strains (Formoso et al., 2015).

In the case of the enzyme 3-hydroxy-3-methylglutaryl coenzyme A reductase (HMG R), a crucial regulator in sterol biosynthesis, exhibits distinct characteristics in the halophilic black yeast *H. werneckii* compared to the well-established eukaryotic model organism, *S. cerevisiae*. This extremophilic eukaryote showcases a unique approach to regulating sterol biosynthesis, a fundamental metabolic pathway in all eukaryotes, diverging from the methods observed in *S. cerevisiae*. Consequently, *H. werneckii* emerges as a valuable model organism for investigating salt stress-responsive proteins and exploring sterol biosynthesis. (Petrovič et al., 1999)

In another study of *Hortaea werneckii* strains, it was observed that proteolytic activities on casein weakened with 5% and 10% NaCl at 25°C for 60% of the strains. Conversely, proteolytic activities on gelatine increased with NaCl. Esterase activities remained positive for all strains at 25°C, even with 5% and 10% NaCl, but were inhibited at 37°C with the addition of 10% NaCl (Zalar et al., 2019c).

2.3 Pigment production by *Hortaea werneckii*.

Structural examinations of the *H. werneckii* cell wall provided insights into its capability for dihydroxy naphthalene (DHN) melanin synthesis under both saline and non-saline growth conditions. However, the arrangement of melanin granules within the cell walls was markedly influenced by salt, indicating a potential osmoprotective function of melanin at the cellular level (Gunde-Cimerman & Plemenitaš, 2006). This phenomenon enabled *H. werneckii* to effectively reduce the permeability of the cell wall to the principal compatible solute glycerol by diminishing pore size.

In the UV absorption spectrum, melanin displayed an absorption peak of maxima ranging from 235 nm to 300 nm (Helan et al., 2013). The UV absorption characteristics of melanin from *H. werneckii* AS1, with a maximum point at 240 nm, aligned with UV spectra observed

in melanins from various fungi and bacteria. Additionally, the IR spectrum of the pigment derived from *H. werneckii* AS1 revealed prominent peaks at approximately 3438.31 cm⁻¹, 2927.31 cm⁻¹, 1637.53 cm⁻¹, and 1239.90 cm⁻¹ indicating (-OH) and aliphatic (C-H) groups, aromatic ring (C=C) stretching, and phenolic (-OH) groups' vibration. These features closely resembled the typical structure of melanin, consistent with pigments reported in various microorganisms (Elsayis et al., 2022). Melanin also shows antibacterial activity against various pathogenic microorganisms.

2.4 Antimicrobial activities of Halotolerant yeast.

The melanin pigment from black yeasts was identified as the primary bioactive compound responsible for antibacterial activity. Various strains were found to produce diverse compounds with antibacterial properties. In the absence of melanin, bioactive compounds with inhibitory activity, including 4-acetoxy-2-azetidinone, sec-butyl-nitrite, octadecadiynoic-acid-methyl-ester, and aspidofractinin-3-ylmethanol, were identified. Furthermore, an elevated level of the alkaloid compound aspidofractinin-3-yl methanol was observed in different strains. This compound has been utilised in the development of antibacterial drugs like quinolones, which play a crucial role in inhibiting bacterial nucleic acid synthesis. (Hodhod et al., 2020).

The melanin pigment exhibited antibacterial effectiveness against *Salmonella typhi*, *Vibrio parahaemolyticus*, and *Klebsiella pneumonia* (Helan et al., 2013). It also demonstrated efficacy against *Escherichia coli*, *Lactobacillus vulgaris*, *Staphylococcus aureus*, *Proteus mirabilis*, *Vibrio cholera*, *Salmonella typhi*, *Salmonella paratyphi*, and *Klebsiella oxytoca*, while having no impact on the tested *B. subtilis* (Kejžar et al., 2013), *L. monocytogens*, *S. pneumoniae*, *K. pneumoniae*, and *P. aeruginosa* strain (Hodhod et al., 2020).

2.5 Exopolysaccharides production by yeasts

Many microorganisms can synthesize exopolysaccharides (EPS), which can be secreted from cells in either soluble or insoluble forms. These EPS serve not only to safeguard the microorganisms but also find diverse applications in biotechnological fields such as pharmaceuticals, textiles, cosmetics, food, metal mining, oil recovery, and metal recovery (Satpute et al., 2010). Consequently, microbial exopolysaccharides have garnered substantial attention from both scientific and industrial communities, emphasizing the importance of identifying microorganisms abundant in these bioactive compounds (Jensen and Fenical, 1996). Despite this, yeasts remain relatively underexplored as producers of exopolysaccharides with novel functional properties and applications. Given their ability to proliferate rapidly on cost-effective substrates in fermenters, yeasts offer ease of large-scale production (Druvefors, 2004). For instance, Chi et al. successfully isolated *Yarrowialipolytica* strains with high protein content from yeasts sourced from diverse marine environments in 2007, while Sheng and Bao (2010) identified 132 yeast strains from grapes, of which three were confirmed as high exopolysaccharide producers.

2.6 Composting using microbial inoculation.

Composting stands as a pivotal technology for treating and transforming organic waste into value-added products. The lignocellulosic composition of biomass waste, such as wood and straw, consisting roughly of 40% cellulose, 20–30% hemicelluloses, and lignin, poses challenges for rapid decomposition in conventional composting processes and often requires an extended timeframe. However, the introduction of bacteria and fungi capable of breaking down lignocellulosic material has shown effectiveness in composting. For instance, the addition of diverse microorganisms such as *Bacillus casei*, *Lactobacillus buchneri*, *Candida rugopelliculosa*, along with lignocellulolytic fungi like *Trichoderma* species and white-rot

fungi, has been observed to expedite the humification and maturation processes during composting.

Among the bacteria involved, *Bacillus* species are prominent, comprising up to 87% of bacteria in thermophilic composts. *Thermus* species exhibit remarkable temperature tolerance, surviving in environments as hot as 65–82°C. *Actinomycetes*, including representatives like *Nocardia*, *Streptomyces*, *Thermoactinomyces*, and *Micromonospora*, are also thermophilic bacteria isolated from compost and recognized for their significant role in lignocellulose degradation. *Trichoderma* species, commonly found in soil, contribute to the degradation of hemicelluloses, aiding in compost stabilization and accelerating the decomposition of waste material.

Recent investigations have focused on exploring the impact of microbial supplementation on composting agro-industrial waste, highlighting microbial inoculation as a viable approach for enhancing organic material biotransformation during composting processes (Zainudin et al., 2022).

2.7 Dyeing of fabrics using pigments from microorganisms.

In the fabric dyeing process, factors such as pH, temperature, and mordants exert significant influence on the efficacy of dyeing. A study investigating fungal pigment dyeing revealed notable effects of pH variations on dye bath characteristics. As the pH values of the dye bath increased from 2 to 5, the colour strength values of each pigment also increased. However, when the pH exceeded 5, the uptake of pigment by cotton yarn markedly decreased. This pH-dependent effect can be attributed to the interaction between the pigment structure and cotton yarn. The anionic nature of the pigment, combined with ionic forces upon binding to the fibre, enhanced the dye ability of the yarn, with optimal pigment uptake observed at pH 5 due to stable pigment colouration. Beyond pH 5, diminishing protonated terminal amino groups

resulted in decreased ionic interaction between the pigment and cotton yarn, reducing dyeability. Furthermore, in the absence of salt, higher colour strength was observed across all pigments, while increasing salt concentration led to decreased colour strength. Dyeing temperature also influenced colour strength, gradually increasing up to 80°C, reaching maximum values. Dyeing at different time intervals revealed a progressive rise in pigment uptake, with maximum uptake percentages observed at 90 min. Cotton, composed primarily of cellulose with reactive hydroxyl groups, exhibits excellent water absorption due to its negatively charged OH groups. The presence of mordants enhances the positive charge of cotton yarn, facilitating faster pigment binding. However, increasing mordant concentration did not consistently yield higher shade depths and could lead to pigment precipitation and uneven dyeing. (Velmurugan†et al., 2010)

CHAPTER 3

METHODOLOGY

3.1 Physiological studies of Halotolerant yeast SPDM15.

3.1.1 Purification and Maintenance of yeast isolate SPDM 15: -

Yeast culture: SPDM15 was received from the guide's culture collection isolated by Ms. Sristi Parsekar using the crude salt sample from Ribandar salt pans at Goa. Isolated colonies were picked up and purified by repetitive subculturing on NaCl Tryptone Yeast Extract (NTYE) agar (Raghavan and Furtado ,2004) containing chloramphenicol (25 mg/ml).

3.1.2 Growth studies of the isolate SPDM15 at varying salt concentrations:

Flasks containing 50 ml of NTYE broth with varying salinity (0%, 5%, 10%, 15%, 20%, 25%, and 30%) were made and inoculated with the SPDM15 isolate and incubated at 28°C ± 30°C for 5 days. The absorbance was taken at 600nm after a gap of 24 hours.

3.1.3 Growth studies of the isolate Yeast SPDM15

SPDM15 was inoculated in 50 ml NTYE broth containing 10% salt concentration. The ingredients of the media included magnesium sulfate heptahydrate (MgSO₄.7H₂O), potassium chloride, tryptone, yeast extract, and agar (1.5-2%). Crude salt was used to attain the respective salinity concentration by filtering it. Chloramphenicol (25 mg/ml) was added to avoid bacterial contamination. The culture growth was observed for 11 days (264hrs) by taking absorbance reading using ShimadzuUV-Vis Spectrophotometer at 600 nm.

3.2 Morphological studies of Halotolerant yeast SPDM15.

3.2.1 Microscopic analysis of SPDM15:

The isolate SPDM15 was grown at different salt concentrations (0%, 5%, 10%, 15%, 20%, 25%, and 30%) in NTYE broth. The SPDM15 culture broth was centrifuged at 10,000 rpm for 10 minutes. The pellet was washed with solutions of respective salt concentrations. The

cells were stained with the lactophenol cotton blue stain on the clean, grease-free slide and observed under a light microscope (100x).

3.2.2 Scanning electron microscopic analysis:

Yeast cells were analyzed by scanning electron microscope using Carl-Zeiss scanning electron microscope (SEM) at Goa University (USIC) to study the morphology at 10% salt concentrations. SPM15 was grown in NTYE broth supplemented with 10% crude salt for a week. One mL of culture broth was centrifuged at 10,000 rpm for 10 minutes. The obtained cell pellet was washed twice with respective salt concentrations and suspended in a sodium phosphate buffer. Loopful of the yeast culture was taken on a grease-free glass slide and allowed to air dry. A drop of 2.5% glutaraldehyde was added to the slide and kept overnight. The next day, the sample was treated with 10%, 30%, 50%, 70%, 90%, and 100% ethanol for 10 minutes. The slide was air-dried. The isolate SPDM 15 sample was analysed by Zeiss EVO 18 special edition after sputter coating.

3.3 Viable cell count of yeast cells.

The isolate was grown in 10 % salt conc. NTYE broth for 5 days, and the absorbance was taken following the incubation. The 100µl of broth was taken and serially diluted using sterile saline from 10^0 to 10^6 . Then 100ul of each dilution was spread plated on a 10% NTYE agar plate and incubated for 3 days. After incubation, the colonies in each dilution plate were counted, and CFU/ml was calculated using the formula below:

$$\text{CFU/ml} = \frac{\text{Number of colonies} \times \text{dilution factor}}{\text{volume of culture plated in ml}}$$

3.4 Molecular identification of the isolate using sequencing approach: -

SPDM15 culture was grown in NTYE agar containing 25% crude salt concentration for 7 days. The isolate was sent for sequencing at Eurofins Genomics India Private Ltd.

3.4.1 Phylogenetic analysis of the isolate SPDM15: -

A. Nucleotide BLAST: -

The consensus sequence was (<https://bioedit.software.informer.com/7.2/>) made by using BioEdit 7.2. BLAST ([https://blast.ncbi.nlm.nih.gov/Blast.cgi?PROGRAM=blastn&BLAST SPEC=GeoBlast&PA GE_TYPE=BlastSearch](https://blast.ncbi.nlm.nih.gov/Blast.cgi?PROGRAM=blastn&BLAST_SPEC=GeoBlast&PA_GE_TYPE=BlastSearch)) was run by using the Standard database. Search was optimized to highly similar sequences (megablast). The species chosen were showing query cover more than 10%. FASTA sequences were downloaded.

B. Phylogenetic tree: -

For building of phylogenetic tree was made using Mega 11 software (<https://www.megasoftware.net/>). The alignment was done using Clustral W and then saved in mega format. To make the phylogenetic tree, neighbor joining tree statistical method was used. Test of phylogeny was bootstrap method and no. of replications were chosen 1000. Kimura 2- 2-parameter model was used. The number of threads was chosen as 8, and the phylogenetic tree was made.

3.5 Test of Pathogenicity for SPDM15:

3.5.1 Test for Hemolysis

40 grams of blood base was mixed with 1 litre of distilled water, and the mixture was heated to a boiling point until complete dissolution occurred. For preparation blood agar, blood base media was cooled to 45-50°C and aseptically 5% of sterile defibrinated blood was added.

Complete lysis of RBCs indicated beta hemolysis, no lysis indicated gamma hemolysis and green or brown discoloration indicated alpha hemolysis (Carrillo et al. 1996).

3.6 Screening of bioactive molecules from SPDM15

The various bioactive molecules screened from SPDM15 were pigment and enzymes. Also the isolate SPDM15 was checked for production of Exopolysaccharides and Biosurfactant.

3.6.1 Pigment analysis of isolate SPDM15:

A) Extraction of pigment from SPDM15

Pigment was extracted from isolate SPDM15 after growing it for a week in 50 ml of NTYE broth with 10% salinity. The culture broth was centrifuged at 10,000 rpm for 10 mins. The supernatant was discarded, and the pellet was rinsed with distilled water two times. Five ml of 1N NaOH was added and autoclaved for 20 mins at 121°C for 15 psi pressure. The obtained mixture was centrifuged at 8000 rpm for 10 mins to separate the black-coloured pigment-containing supernatant. The supernatant containing melanin pigment was transferred to sterile tubes. By using concentrated HCl supernatant was acidified to pH 2 followed by centrifugation at 8000 rpm for 10 mins. The supernatant was thrown, and the pellet was rinsed four times with distilled water, followed by drying in a dehumidified environment overnight and stored at 4°C for further analysis.

B) Partial characterization of pigment using Fourier- Transform infrared (FTIR) analysis:

The pigment in powder form was processed for FTIR analysis. The sample was analyzed using a Bruker Alpha II FTIR spectrophotometer. Origin pro software (<https://www.originlab.com/origin>) was used to visuals and plot the data.

3.6.1.1 Dyeing of cotton cloth using melanin pigment:

A) Initial treatment of Cotton fabric

One gram of cotton fabric was cut into pieces and was treated in boiling water containing 5g/l of sodium lauryl sulphate for 1hr. The cloth was removed, washed sequentially with hot and cold water, squeezed, and air dried at room temperature. This was followed by treatment with 1M HCl at room temperature for 30 minutes and then washing with deionized water until the rinsed water was neutral. (Velmurugan†et al.,2010)

B) Pre mordanting of fabric

The fabric pieces were boiled in different mordants as per Table 1 at 70°C for 1hr in a beaker. Then thefabrics were left in the beaker at room temperature overnight. Then squeezed to remove excess liquor and air dried at room temperature overnight. (Velmurugan†et al.,2010)

Table1: Different types of mordants used for post and pre-mordanting of cotton fabric	
Natural mordants	5% Alum, 5% Aloe vera, and 5% Lemon,
Synthetic mordants	5% Cupric Sulphate, 5% Potassium dichromate, 5% Ferrous Sulphate
Combination of different mordants	5% Alum + 0.03g Sodium carbonate, 0.03g Ferrous sulphate + 5% Alum, 5% Alum + 10% Lemon, 5% Alum + 10% Aloe vera

C) Dyeing of cotton fabric

The different pre-mordant treated cotton cloth weighing total of 1g was labelled and dyed with extracted pigments in a round bottom flask containing 1 g pigment in 100 ml deionized water with 0.15g sodium sulfate at 80 °C for 90 min in a Rotary evaporator operated at 150 rpm

D) Post-mordanting of Fabric

The dyed cotton yarn was impregnated with the previously mentioned respective mordant solutions at room temperature for 30 min. The cotton yarn was removed, washed with water to remove the unfixed dye, and then air-dried at room temperature overnight to dry.

3.6.1.2 Colour Fastness Test of Cotton Fabric

A) Determination of Light Fastness Properties on Dyed Cotton Fabrics

After dyeing the cloth, it was exposed to sunlight for 2 hours and the change in colour was observed.

B) Determination of Washing Fastness Properties on Dyed Cotton Fabrics

After dyeing the cloth, it was washed in detergent for 30 mins followed by rinsing with water and the change in colour was observed

C) Determination of Wet rubbing Fastness Properties on Dyed Cotton Fabrics

After dyeing the cloth, it was rubbed with a standard white cloth with water content is 95% to 105% and the change in colour was observed

3.6.1.3 Antibacterial activity of dyed and undyed cotton fabric

Antimicrobial properties of the melanin pigment in the study were tested against *Salmonella typhi*, *Klebsiella pneumonia* and *Providencia rettgeri*. To check antimicrobial activity, agar disc diffusion method was carried out (Kirby-Bauer method) (Bauer, Kirby 1961). The pure cultures of the pathogens were prepared in suspension using sterile saline and were spread plated on Mueller-Hinton agar plates using a sterile swab under aseptic conditions in a Laminar Airflow Chamber. The culture was allowed to get absorbed by the media by letting the plates rest for 5-10 minutes. Then, a sterile dyed cloth piece in which mordant alum + sodium carbonate was utilized was placed on the plates and incubated for 24 hrs. at 37°C. undyed cloth piece mordanted with sodium carbonate + alum was used as a control. After incubation, the zone of clearance was noted down.

3.6.2 Screening of SPDM15 isolate for Enzyme involved in plant polymer degradation:

The following enzymes screened from SPDM15 are as follows:

A) Amylase

SPDM15 was spot inoculated on NTYE agar containing 10% crude salt and 2% soluble starch. Plates were incubated at $28^{\circ}\text{C} \pm 30^{\circ}\text{C}$ for 7 days. Following the incubation period, the plates were flooded with an iodine solution (0.2% iodine, 0.4% KI, 100 ml H₂O) and examined for the presence of clear zones surrounding the colonies.

B) Cellulase

SPDM15 was spot inoculated on an NTYE agar plate supplemented with 2% Carboxy Methyl Cellulose (CMC) and 10% crude salt. Plates were incubated at $28^{\circ}\text{C} \pm 30^{\circ}\text{C}$ for 18-20 days. After incubation, the plates were saturated with 0.1 per cent (w/v) Congo red (Sethi et al., 2013). The formation of a clear zone around the culture indicated cellulase production.

C) Protease

SPDM15 was spot inoculated on a 2% skimmed milk NTYE agar plate. The plates were incubated for 7 days at $28^{\circ}\text{C} \pm 30^{\circ}\text{C}$. The plates were observed for the formation of a halo/clearance zone after incubation.

D) Esterase

SPDM15 was spot inoculated NTYE agar plate supplemented with 1% Tween 80 and 10% crude salt. The plates were incubated for 7 days at $28^{\circ}\text{C} \pm 30^{\circ}\text{C}$. After incubation, the presence of whitish halos around the colony indicated a positive result.

E) Pectinase

SPDM15 was spot inoculated on 2% pectin NTYE agar plate containing 10% crude salt. The plates were then incubated for 7 days at $28^{\circ}\text{C} \pm 30^{\circ}\text{C}$. After incubation, the plates were flooded with 1% hexadecyltrimethylammonium bromide, and a clear halo around the colony indicated a positive result. (Buzzini et al., 2002)

F) Gelatinase

SPDM15 was spot inoculated on 2% Gelatin NTYE broth containing 10% crude salt. The tubes were incubated for 7 days at $28^{\circ}\text{C} \pm 30^{\circ}\text{C}$. After incubation, the tubes were kept at 4°C for 24 hrs. Liquefaction at 4°C after 24 hrs. indicated positive result.

G) Urease

SPDM15 was spot inoculated on 2% urea NTYE agar slants containing phenol red, 5% and 10% crude salt. The tubes were incubated for 7 days at $28^{\circ}\text{C} \pm 30^{\circ}\text{C}$. After incubation, the tubes were examined for a colour change from yellow to pink, indicating urease activity.

H) Agarase

SPDM15 was spot inoculated on seawater NTYE agar plate. After incubation for 7 days at $28^{\circ}\text{C} \pm 30^{\circ}\text{C}$, the plates were flooded with Lugol's iodine to check for zone of clearance around the colonies.

I) Catalase

SPDM15 was spot inoculated on glass slide with a drop of 3% hydrogen peroxide. Effervescence indicated positive result.

J) Lipase

SPDM15 was spot inoculated on tributyrin agar supplemented with 2% tributyrin (Atlas et al., 1993), 10% crude salt, magnesium sulfate heptahydrate, potassium chloride and tryptone. Plates were then incubated for 4 weeks at $28^{\circ}\text{C} \pm 30^{\circ}\text{C}$. After incubation, zone of clearance around the colony indicated positive result.

K) Laccase

SPDM15 was spot inoculated on NTYE agar plates containing 0.01 % sterile ABTS. The plates were then incubated for 3 weeks at $28^{\circ}\text{C} \pm 30^{\circ}\text{C}$. After incubation, dark green halo around the yeast growth colony indicated positive result.

L) Xylanase

SPDM15 was spot inoculated on an NTYE agar plate containing 2% Xylan and 10% crude salt. After incubation for 7 days at $28^{\circ}\text{C} \pm 30^{\circ}\text{C}$ the plates were observed for zone of clearance around the colonies indicating positive result.

3.6.3 Exopolysaccharides Screening Test:

Yeast isolate was streaked on Congo red agar plates supplemented with 5% sucrose, 10% crude salt for the detection of exopolysaccharides produced. The plates were incubated for 3 days at $28^{\circ}\text{C} \pm 30^{\circ}\text{C}$. Production of exopolysaccharides is confirmed by formation of black and opaque colonies on Congo red Agar plates.

3.6.4 CTAB-methylene blue agar test for Biosurfactant production.

The CTAB-methylene blue agar test was assessed using an agar well diffusion assay method outlined by Siegmund and Wagner (1991). The NTYE medium was enriched with Cetyltrimethylammonium bromide (CTAB) at a concentration of 0.2 g/L, methylene blue at 0.005 g/L, and agar at 17 g/L. Wells measuring 8 mm in diameter were created at the center of the CTAB-methylene blue agar plates using a sterile cork borer. 100 μL of yeast cultures were added to each well. The plates were incubated at $28^{\circ}\text{C} \pm 30^{\circ}\text{C}$ for 7–8 days. Positive results were recorded as a dark blue halo and a yellow zone of clearance around the colony.

3.7 Accelerating the composting process using SPDM15 as a bio inoculum.

Six raw materials such as leaves, paper, food waste, sawdust, grass clipping and soil were used for the composting experiment. Different substrates were added to each container, as shown in Table 2, and the C:N ratio was maintained between the range 30:1-20:1. Water was added occasionally to maintain the moisture to 45%-70%, and stirring of the waste was done twice a week. PH, ash, Volatile Solids, and Total Solids were initially measured. The temperature was monitored daily.

Different raw materials were weighed and incorporated into various compost sets such as T1, T2, T3, T4, T5, and T6. In T1, T2, and T3, quantities of 325g, 12g, 8g, 18g, and 1437g of leaves, paper, sawdust, grass clippings, and food waste were added, respectively. In T4, T5, and T6, quantities of 435g, 6g, 4g, 18g, and 1097g of leaves, paper, sawdust, grass clippings,

and food waste were added, along with 240g of soil. In T4, autoclave soil was used, whereas in T5 and T6 non, autoclaved soil was used. Additionally, in T2, T5, 10^9 CFU/g of yeast culture was added once, while in T3, it was added thrice till the compost maturity.

Table 2:-Combinations of raw materials for the Composting process

Raw material	T1 (g)	T2 (g)	T3 (g)	T4 (g)	T5 (g)	T6 (g)
Leaves	325	325	325	435	435	435
Paper	12	12	12	6	6	6
sawdust	8	8	8	4	4	4
Grass clippings	18	18	18	18	18	18
Food waste	1437	1437	1437	1097	1097	1097
soil	-	-	-	240	240	240
Total weight	1800					

3.7.1 Analysis of Compost for various parameters:

A) pH analysis

To find at which stage the compost has reached, it is essential to measure the pH. The compost was digested using water in the ratio 1 10 (compost/water) using an orbital shaker, and the pH was measured.

B) Total solid, volatile solid, Ash, and moisture content analysis

The crucible was washed with tap water and dried in the oven to remove moisture. The weight of the crucible was noted after drying the crucible. Compost was added to the crucible, and weight was measured (W2). This was kept in the oven at 105°C overnight. After drying in the oven, the crucible was cooled in the desiccator, and weight was measured (W3). Later the crucible was kept in a furnace for two hours incubation at 550°C. After cooling down the crucible weight was measured (W4).

The total solid, volatile solid, Ash and moisture content was estimated by substituting the above obtained values in the formula mentioned below:

FORMULA

W1 =dry crucible weight

W2=weight of sample + crucible

W3=weight of crucible after drying at 105°

W4=weight of crucible after drying at 550°

Moisture= $W2 - W3 / \text{weight of sample} \times 100$

TS = $W3 - W1 / \text{Weight of sample} \times 100$

VS = $W3 - W4 / \text{Weight of sample} \times 100$

Ash = $W4 - W1 / \text{weight of sample} \times 100$

C) Temperature analysis

The temperature of different sets of compost were recorded for 20 days using thermometer.

3.7.2 Phytotoxicity Analysis of Compost

Compost samples (T1, T2, T3, T4, T5 and T6) , Market compost (MC), Compost T3 with 200ul of SPDM15 (T7) , Soil and Tap water (control) were used for the experiment. 5g of Compost Samples, T7, Market compost and soil were mixed with 50ml of water in their respective flasks. The mixture were then kept on the shaker for 15 minutes. The samples were then filtered with Whatman filter paper grade 42. Cowpea (*Vigna unguiculata*) seeds were used for the experiment. The seeds were thoroughly washed with distilled water and surface sterilized using 2% of sodium hypochlorite for 1 min. Subsequently, seeds were washed four times in sterile distilled water and air-dried under a laminar flow hood. Then, 5 sterile Cowpea seeds were placed in each sterile petri plate labelled T1, T2, T3, T4, T5,T6, T7, MC and soil on absorbent cotton and 10 ml of respective extract was added to it. The control plate used 10 ml of tap water instead of the extract mixture. Petri dishes were incubated in the dark for 72 hrs. After 72 hours of incubation, the germination rate and Vigor index were calculated.

$$\text{Germination rate (\%)} = (\text{Total number of germinated seeds} \div \text{Total number of seeds}) \times 100$$

$$\text{Vigor index} = \text{Germination rate (\%)} \times \text{Total seedling length (cm)}$$

3.7.3 CHNS analysis of different compost sets to evaluate the maturity of compost

The 25th-day compost samples (T1, T2, T3, T4, T5 and T6) in dried powdered form were sent for CHNS analysis. The sample was analyzed through CHNS Elemental Analyzer of model Elementar Vario Micro Cube.

CHAPTER 4

ANALYSIS

AND

CONCLUSIONS

4.1 Growth Studies of isolate SPDM15 at various salt concentrations:

Isolate SPDM15 was grown in NTYE broth for 3 days and its growth rate was calculated. The results indicated a correlation between salinity and growth. Analysis of the data revealed that, at a 0% salt concentration, the growth rate was low in the absence of salt in the medium. The highest growth rate was observed at a 10% salt concentration, followed by a subsequent decrease in growth rate with an increase in salinity. The lowest growth was recorded at a 30% salt concentration. Studies showed that the growth is stimulated by the salinity at 5% salt concentration and it was capable to grow at higher salinities (Kogej et l., 2005). **Table 3** depicts the growth studies of SPDM15 at various salt concentrations. **Fig 1** shows the graphical representation of data from table 3.

Salt concentration (%)	O.D at 600nm
0 %	1.14
5%	2.804
10%	3.328
15%	2.362
20%	0.8765
25%	0.278
30%	0.136

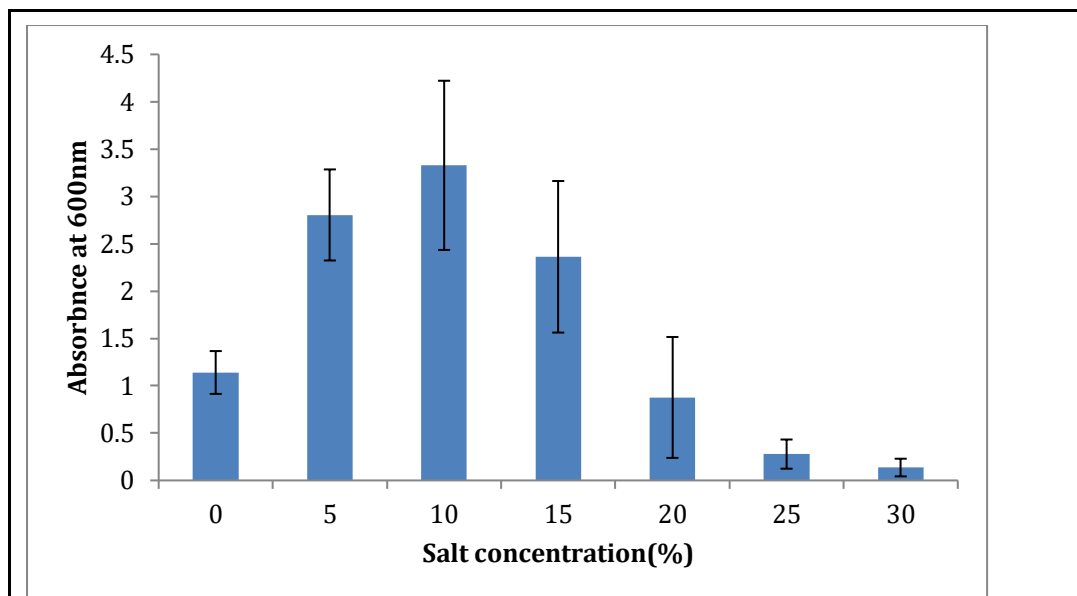


Fig 1: The growth studies of isolate SPDM15 was measured at various salt concentrations at room temperature.

There was an increase in the yeast growth from 0% to 15%, and after that, there was a sharp decrease in it showing that at higher salt concentrations growth decreases. As studies show that addition of the 20% salt decreased growth of *H. werneckii* (Kogej et al., 2005). Also, it is reported that Growth of *H. werneckii* increases from 0% to 10%, it is stable in between 10% to 20% and it decreases above 20% (Plemenitas& Gunde-Cimerman, n.d.).

Non-adapted cells lose turgor and volume when exposed to high salt concentrations, but adapted fungal cells selectively absorb suitable solutes. This process is known as a hyperosmotic shock, and it is followed by a quick osmotic adjustment (Blomberg & Adler, 1992; Plemenitaš& Gunde-Cimerman, n.d.). Intriguingly, K^+ and Na^+ concentrations in *H. werneckii* cells cultured at 17% NaCl were the lowest. Although *H. werneckii* continues to grow effectively at this medium salinity, 17% NaCl most likely marks a turning point for this organism as evidenced by *H. werneckii*'s small colony size, reduced growth rate, and distinctive alterations in physiological behaviour (Plemenitaš& Gunde-Cimerman, n.d.)

4.1.1 Growth studies of isolate SPDM15 at 10% crude salt concentrations in NTYE media:

Yeast cells were grown in NTYE broth at 10% salt concentration. Absorbance was taken at 600 nm after every 24 hours. Absorbance at 10% salt concentration in NTYE broth for 11 days is depicted in **Table 4**. The graphical representation of data in Table 4 is depicted in **Fig 2**.

Table 4: Absorbance at 10% salt concentration for 11 days.

Time of incubation	O.D at 600nm
24hr	0.034
48hr	0.108
72hr	0.802
96hr	2.728
120hr	3.739
144hr	4.794
168hr	5.64
192hr	7.530
216hr	6.669
240hr	6.603
264hr	6.128

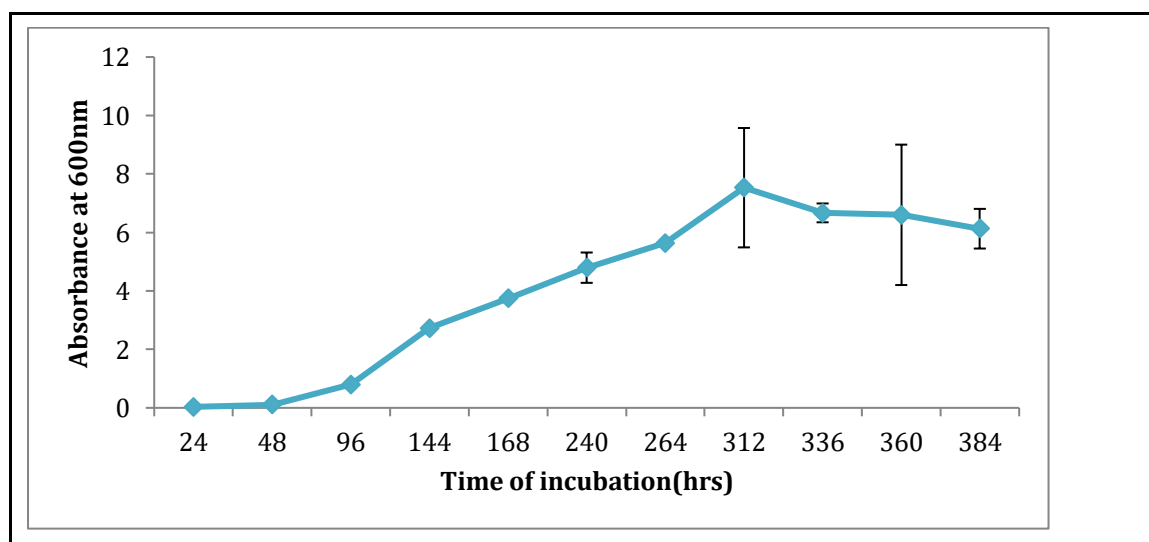


Fig 2: Optical density measurement after every 24hrs of isolate SPDM15 in presence of 10% salt concentration in NTYE broth.

Isolate SPDM15 was grown at 10% salt concentration NTYE broth from 24 hrs to 384 hrs of incubation and its absorbance was measured at 600 nm. The turbidity of the broth on the third day following inoculation indicated that there was evident growth in the medium. Absorbance started increasing from the 2nd till 8th day showing an exponential rise. From the 9th day, there was decrease in the absorbance showing a stationary phase

4.2 Microscopic analysis of isolate SPDM15:

Isolate SPDM15 changes morphology at different salt concentration hence microscopic analysis was done by lactophenol Cotton Blue Stain. **Fig 3 (A to G)** depicts Fig A, B, C, D, E, F and G indicating the different forms of yeast seen in 0%, 5%, 10%, 15%, 20%, 25% and 30% salt conc. respectively.

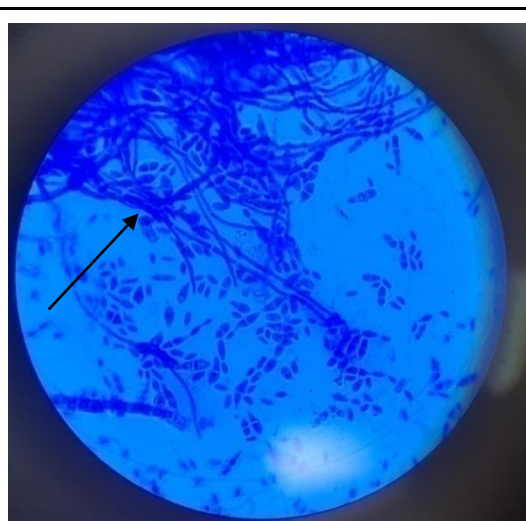


Fig: A(0% salt conc , Filamentous hyphal structure surrounded by isolated cells)

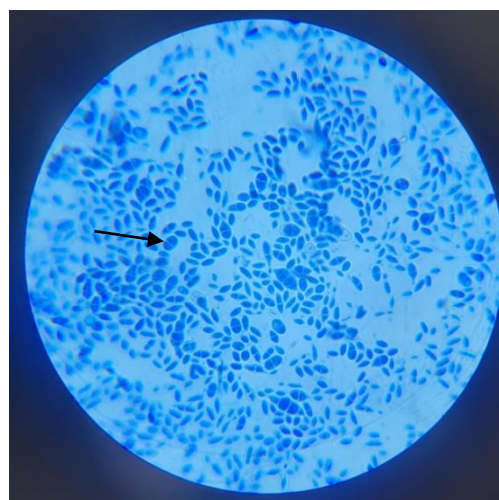


Fig: B (5% salt conc, yeast with two celled structure)

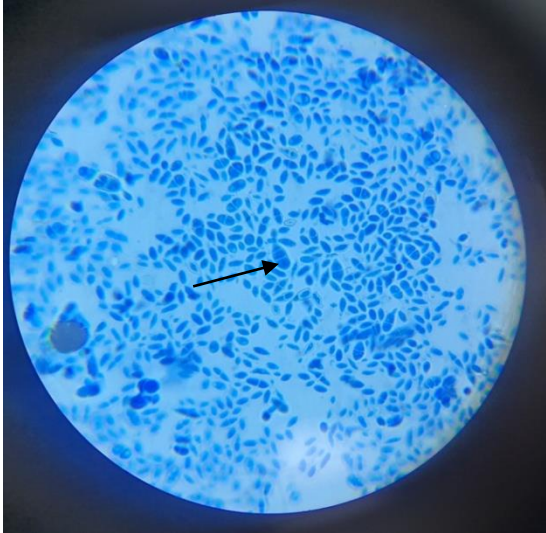


Fig: C (10% salt conc, yeast with three celled structure)

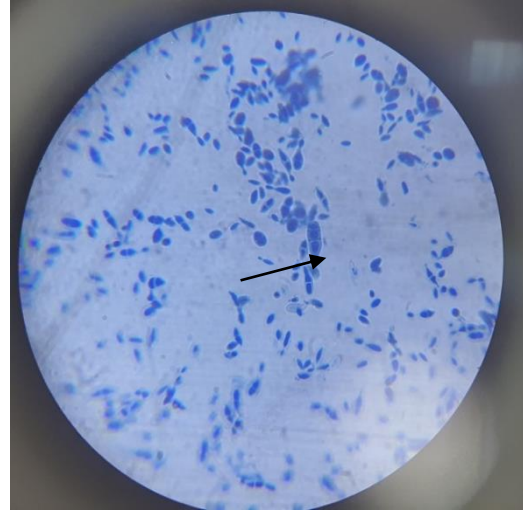


Fig: D (15% conc, three celled structure showing polar budding)



Fig: E (20% salt conc, bipolar budding)

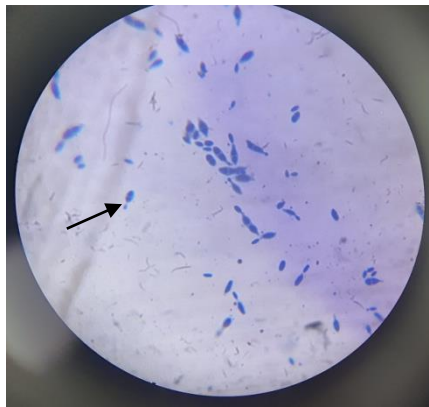


Fig: F (25% salt conc, polar budding)



Fig:G (30% salt conc, isolated yeast cell showing polar budding)

Fig 3(A to G): Morphology of isolate SPDM15 grown in NTYE broth at different salt concentrations.

Morphology of isolate SPDM15 at different salt concentrations was observed through lactophenol blue staining. In fig A, at 0% salt concentration, filamentous hyphal structures were observed with budding structures and longitudinal septa. fig B shows a 5% salt concentration, and two-celled concatenated structures were seen. Three-celled structure was observed at 10% salt conc in Fig C. In fig D with 15% salt concentration three celled structure showing polar budding was seen. Bipolar budding was seen in 20% salt concentration in fig E, and polar budding was observed in 25% and 30% salt concentration in fig F and G, respectively.

In a study of the microscopic structures of *Hortaea werneckii*, the dimensions, morphology, and pigmentations of its conidia were observed to be influenced by the specific growth medium, exhibiting variability across different strains. Regardless of the culture media used, initial yeast-like growth was observed in colonies, with subsequent development of superficial, aerial, or immersed mycelia in many instances. The slender hyphae were either comprised of elongated cells or appeared as pseudo mycelia, consisting of concatenated two-celled conidia constricted at the septa. Furthermore, the thicker hyphae were longitudinally septate. The mycelial structures exhibited lateral proliferating openings, which could be nearly sessile, give rise to short single conidiogenous cells or even complex conidiophores forming synnema-like arrangements. Notably, clusters of hyphae resembling sterile 'pseudo' fruiting bodies were observed on oatmeal agar medium. Conidia formation followed annellidic conidiogenesis, typically resulting in one or two-celled melanized conidia with bipolar budding. (Zalar et al., 2019)

4.2.1 SEM analysis of isolate SPDM15:

To understand the morphology and size of the isolate SPDM15, SEM analysis was carried out. **Fig 4** depicts the SEM images of isolate SPDM15 in 10% salt conc. NTYE media.

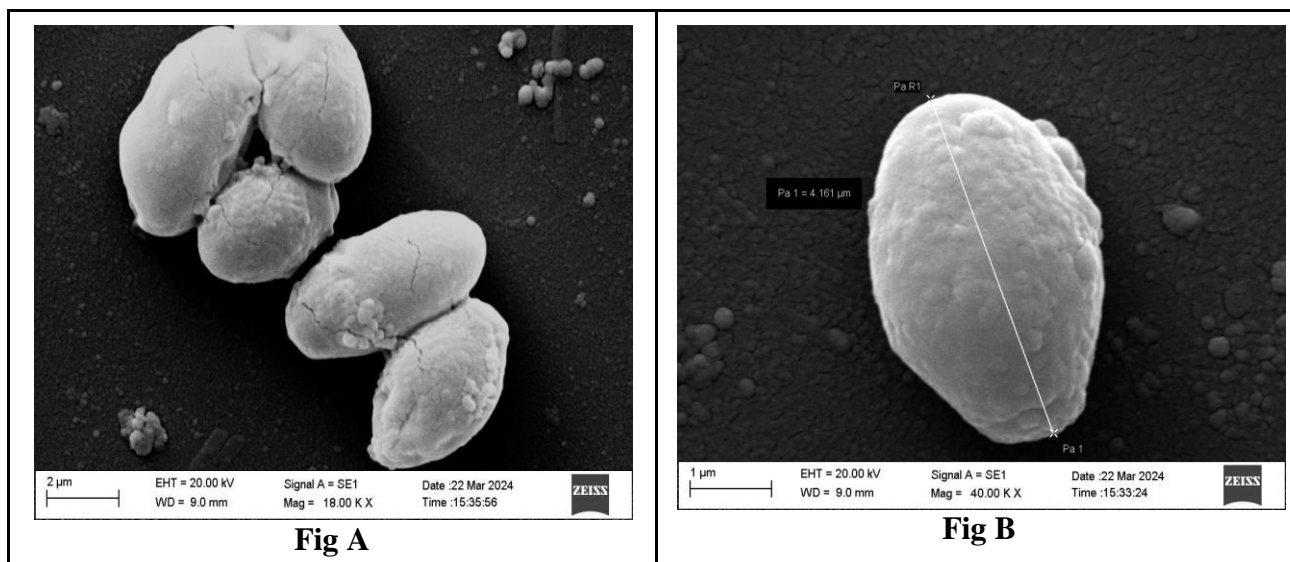


Fig 4: SEM analysis of isolate SPDM15 grown in NTYE broth at 10% salt concentration.

The surface morphology of the colonies was observed by SEM analysis. SPDM15 was observed at a magnification of 18.00 K X revealing structures resembling yeast cells as shown in Fig A. The size of the isolate was found to be 4.161 µm as shown in Fig B.

4.3 Viable yeast cell count on NTYE agar with 10% salt concentration

Viable yeast cell count in NTYE agar with 10% salt concentration was done to check the yeast viability. Fig 5 (A to G) represents Fig A, B, C, D, E, F and G with 10^0 , 10^1 , 10^2 , 10^3 , 10^4 , 10^5 and 10^6 dilutions of isolate SPDM15 after incubation in 10% NTYE broth for 3 days.

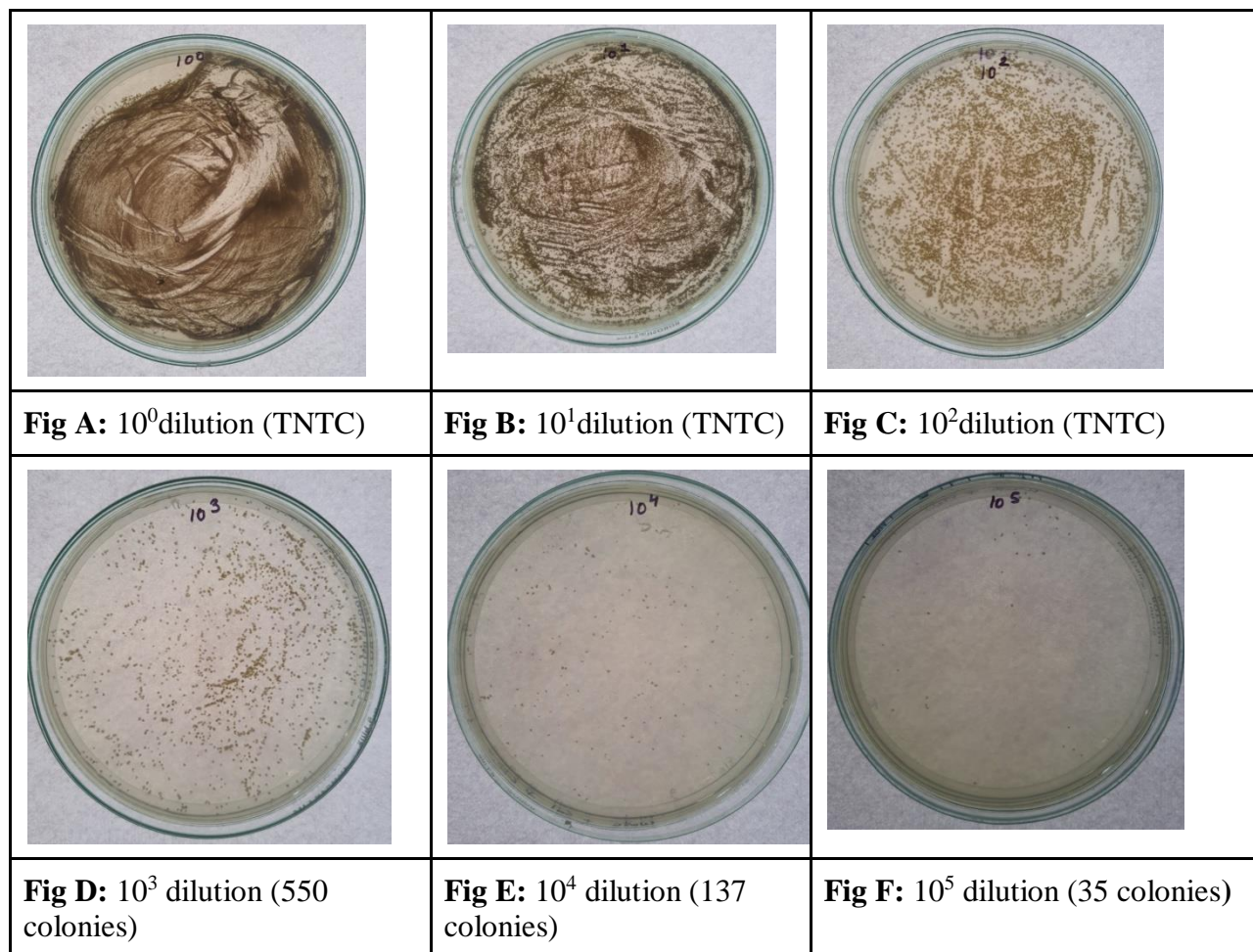


Fig 5 (A to G): Yeast viability (colony forming unit per ml) on 10% NTYE media

The NTYE broth inoculated with yeast culture of absorbance 2.684 was used to check the viability of yeast culture. The sample was diluted from 10^0 to 10^6 . In fig A, B, C and D of

dilution 10^0 , 10^1 , 10^2 , 10^3 were too numerous to count (TNTC) since there were colonies more than 300. Fig G, the plate dilution with 10^6 had 3 colonies and were too few to count (TFTC). Fig E and Fig F, the plate of 10^4 and 10^5 dilution had 137 and 35 colonies respectively. The plate with 10^4 dilution was selected to calculate the CFU/ml since it fell in the range 30 and 300 colonies, ideal for standard plate count. The viable number of colonies was found to be 1.37×10^9 CFU/ml on 10% NaCl Tryptone Yeast Extract (NTYE) agar after 3 days incubation.

4.4 Sequencing of isolate SPDM15

Although morphological traits are helpful for describing species, they may have certain limitations because many macroscopic structures are formed sporadically and briefly (Bickford et al., 2007). In addition to being very promising for identifying species, molecular technologies can be used to accurately and quickly assess biological diversity. Since the 1990s, these markers have been used to identify several fungi species (Blackwell, 2013; Bruns et al., 1991). For a large number of the fungal lineages examined, the internal transcribed spacer (ITS) region of nuclear ribosomal RNA displayed the highest probability of correct identification (PCI) and the most prominent barcode gap (Schoch et al., 2012). The ITS region has since come to be recognized as the typical barcode marker for fungus. This area is not equally variable in all taxa of fungi, according to a detailed analysis of ITS sequences in the International Nucleotide Sequence Database (INSD: GenBank, EMBL, and DDBJ) (Nilsson et al., 2008). The fact that most fungal species have been identified using the ITS region as a standard identifier is one benefit of doing so. GenBank is the most complete and extensively utilised sequence repository (O'Donnell & Cigelnik, 1997).

A) Forward sequence: -

>0922_705___SPDM-15_28S_F_D10.ab1

CAGTCCATTTAGAGACAACAGGGATTGCCCTAGTAACGGCGAGTGAAGCGGCAA
 CAGCTCAAATTTGAAATCTGGCGCAAGCCCGAGTTGTAATTTGTAGAGGATGCTT
 CTGGGCAGCGGCCGGTCTAAGTTCCTTGGAACAGGACGTCATAGAGGGTGAGAA
 TCCCGTATGCGACCGGCTTGCACCCGTCACGTAGCTCCTTCGACGAGTCGAGTTG
 TTTGGGAATGCAGCTCTAAATGGGAGGTAAATTTCTTCTAAGGCTAAATACCGGC
 CAGAGACCGATAGCGCACAAAGTAGAGTGATCGAAAGATGAAAAGCACTTTGGAA
 AGAGAGTTAAAAAGCACGTGAAATTGTTGAAAGGGAAGCTCACGCGGCCGGACT
 TGTCGGCGGTGTTCCGCCGGTCTTCTGACTGGCCTATTCGCCGACGGAAGGCCAA
 CATCACTTGGCAGCGCCGGATCCTCTAGTGATTACAGCACGCCCTCGCGCCATAT
 TACAAATTCGAGCTGTTGCCGCTCCCCTCACCGAGGCCAGGGCAACCGCTGTGGG
 GTTCGTTTCCTCCGCGCATGGAGACGCTCAAGATCCACGGATAGGGAAA

B) Reverse sequence: -

>0922_705___SPDM-15_28S_R_E10.ab1

TTANCCTTTCGCCAGCATCCTAGCCGAAGCGCGGACCTCACTCGGGAGGGCGCCGT
 ATTGTGCGCGCGGCTATAATGCCCCGAGGGGCTACATTCCGCACGCCTTTATCCG
 GCGCTCCCAAGTGATGCTGGCCTGCCGGCGGCGAATAGACCGGTCAGAAGACCG
 GCGGAACACCGCCGACAAGTCTGGTTGCGTGAGCTTCCCTTTCAACAATTTACG
 TGCTTTTTAACTCTCTTTCCAAAGTGCTTTTCATCTTTCGATCACTCTACTTGTGCG
 CTATCGGTCTCTGGCCGGTATTTAGCCTTAGAAGAAATTTACCTCCCATTTAGAG
 CTGCATTCCCAAACAACCTCGACTCGTCGAAGGAGCTACGTGACGGGTGCAAGCC
 GGTCGCATACGGGATCTCACCTCTATGACGTCCTGTTCCAAGGAACTTAGACCG
 GCCGCTGCCCAGAAGCATCCTCTACAAATTACAACCTCGGGCTTGCGCCAGATTC

AAATTTGAGCTGTTGCCGCTTCACTCGCCGTTACTAGGGCAATCCCTGTTGGTTTC
TTTTCTCCGCTTATTGATATGCTTAAATTCAGCGGGTAG

C) Consensus sequence: -

>SPDM15

GAGTGAAGCGGCAACAGCTCAAATTTGAAATCTGGCGCAAGCCCGAGTTGTAAT
TTGTAGAGGATGCTTCTGGGCAGCGGCCGGTCTAAGTTCCTTGGAACAGGACGTC
ATAGAGGGTGAGAATCCCGTATGCGACCGGCTTGCACCCGTCACGTAGCTCCTTC
GACGAGTCGAGTTGTTTGGGAATGCAGCTCTAAATGGGAGGTAAATTTCTTCTAA
GGCTAAATACCGGCCAGAGACCGATAGCGCACAAAGTAGAGTGATCGAAAGATGA
AAAGCACTTTGGAAAGAGAGTTAAAAAGCACGTGAAA

4.4.1 Phylogenetic analysis: -

A. Nucleotide BLAST

Isolate SPDM15 was sent for the rRNA ITS sequencing. To study the species identity and Verification nucleotide BLAST was run by keeping the all parameters default ([https://blast.ncbi.nlm.nih.gov/Blast.cgi?PROGRAM=blastn&BLAST SPEC=GeoBlast&PAGE TYPE=Blast Search](https://blast.ncbi.nlm.nih.gov/Blast.cgi?PROGRAM=blastn&BLAST_SPEC=GeoBlast&PAGE_TYPE=Blast_Search)). Consensus sequence was made by using Bioedit software. Fig 6 shows the significant alignments of isolate SPDM15 showing maximum identity with *Hortaea werneckii* species.

Sequences producing significant alignments		Download	Select columns	Show	100				
Description		Scientific Name	Max Score	Total Score	Query Cover	E value	Per. Ident	Acc. Len	Accession
<input checked="" type="checkbox"/>	Hortaea werneckii strain Al-Sabri-Y13 large subunit ribosomal RNA gene, partial sequence	Hortaea werneckii	573	573	100%	1e-158	100.00%	1324	MN700180.1
<input checked="" type="checkbox"/>	Hortaea werneckii isolate 1Y97 5.8S ribosomal RNA gene, partial sequence: internal transcribed spacer 2, com...	Hortaea werneckii	573	573	100%	1e-158	100.00%	1147	MN401288.1
<input checked="" type="checkbox"/>	Hortaea werneckii isolate 2Y218 large subunit ribosomal RNA gene, partial sequence	Hortaea werneckii	573	573	100%	1e-158	100.00%	879	MN396737.1
<input checked="" type="checkbox"/>	Hortaea werneckii isolate 2Y110B large subunit ribosomal RNA gene, partial sequence	Hortaea werneckii	573	573	100%	1e-158	100.00%	1151	MN396734.1
<input checked="" type="checkbox"/>	Hortaea werneckii isolate 2Y126D large subunit ribosomal RNA gene, partial sequence	Hortaea werneckii	573	573	100%	1e-158	100.00%	1130	MN396733.1
<input checked="" type="checkbox"/>	Halichoeres hortulanus isolate 2Y126C2 large subunit ribosomal RNA gene, partial sequence	Halichoeres hort...	573	573	100%	1e-158	100.00%	1109	MN396711.1
<input checked="" type="checkbox"/>	Hortaea werneckii isolate 2Y126C1 large subunit ribosomal RNA gene, partial sequence	Hortaea werneckii	573	573	100%	1e-158	100.00%	1148	MN396710.1
<input checked="" type="checkbox"/>	Hortaea werneckii isolate 2Y126B large subunit ribosomal RNA gene, partial sequence	Hortaea werneckii	573	573	100%	1e-158	100.00%	1141	MN396709.1
<input checked="" type="checkbox"/>	Hortaea werneckii isolate 2Y126A large subunit ribosomal RNA gene, partial sequence	Hortaea werneckii	573	573	100%	1e-158	100.00%	1167	MN396707.1
<input checked="" type="checkbox"/>	Hortaea werneckii isolate 2Y126E large subunit ribosomal RNA gene, partial sequence	Hortaea werneckii	573	573	100%	1e-158	100.00%	1167	MN396561.1
<input checked="" type="checkbox"/>	Hortaea werneckii isolate 2Y194B large subunit ribosomal RNA gene, partial sequence	Hortaea werneckii	573	573	100%	1e-158	100.00%	1178	MN396534.1
<input checked="" type="checkbox"/>	Hortaea werneckii isolate CON2A9 large subunit ribosomal RNA gene, partial sequence	Hortaea werneckii	573	573	100%	1e-158	100.00%	539	MN307932.1
<input checked="" type="checkbox"/>	Hortaea werneckii strain YH_Yeh V0314 large subunit ribosomal RNA gene, partial sequence	Hortaea werneckii	573	573	100%	1e-158	100.00%	574	MH160818.1
<input checked="" type="checkbox"/>	Hortaea werneckii strain Al-Sabri-Y11 large subunit ribosomal RNA gene, partial sequence	Hortaea werneckii	573	573	100%	1e-158	100.00%	1315	MK541928.1
<input checked="" type="checkbox"/>	Hortaea werneckii culture CBS:126987 strain CBS_126987 large subunit ribosomal RNA gene, partial sequence	Hortaea werneckii	573	573	100%	1e-158	100.00%	896	MH875816.1
<input checked="" type="checkbox"/>	Hortaea werneckii culture CBS:126984 strain CBS_126984 large subunit ribosomal RNA gene, partial sequence	Hortaea werneckii	573	573	100%	1e-158	100.00%	890	MH875814.1
<input checked="" type="checkbox"/>	Hortaea werneckii culture CBS:708.76 strain CBS_708.76 large subunit ribosomal RNA gene, partial sequence	Hortaea werneckii	573	573	100%	1e-158	100.00%	894	MH872799.1
<input checked="" type="checkbox"/>	Hortaea werneckii culture CBS:359.66 strain CBS_359.66 large subunit ribosomal RNA gene, partial sequence	Hortaea werneckii	573	573	100%	1e-158	100.00%	870	MH870461.1

Fig 6: Significant alignments of isolate SPDM15 showing maximum similarity with *Hortaea werneckii* species

After doing alignment by using BLAST. Isolate SPDM15 showed 100 % identity with the various strains of the *Hortaea werneckii* species such as *Hortaea werneckii* strain Al-Sabri-Y13, *Hortaea werneckii* isolate 1Y97, *Hortaea werneckii* isolate 2Y218, and *Hortaea werneckii* strain UWFP 1116. There were more strains of *Hortaea werneckii* showing an identity of more than 100%, shown in the figure above. This confirmed that the isolate SPDM was *Hortaea werneckii*.

.B. Phylogenetic tree

The phylogenetic tree was constructed to identify the closely related species of the isolate SPDM15. **Fig7** depicts the phylogenetic tree of SPDM15 species and related taxa based on the ITS region.

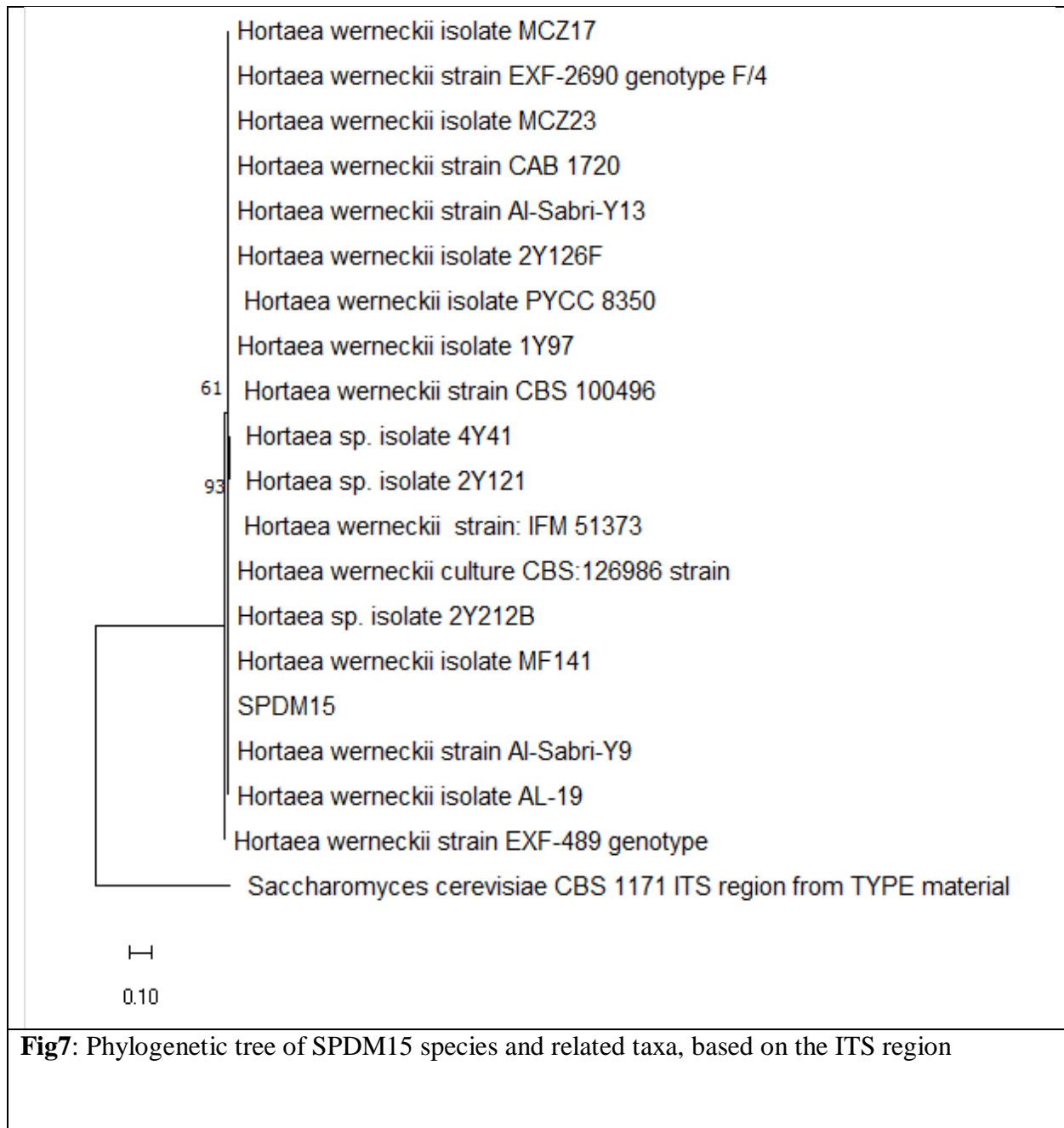


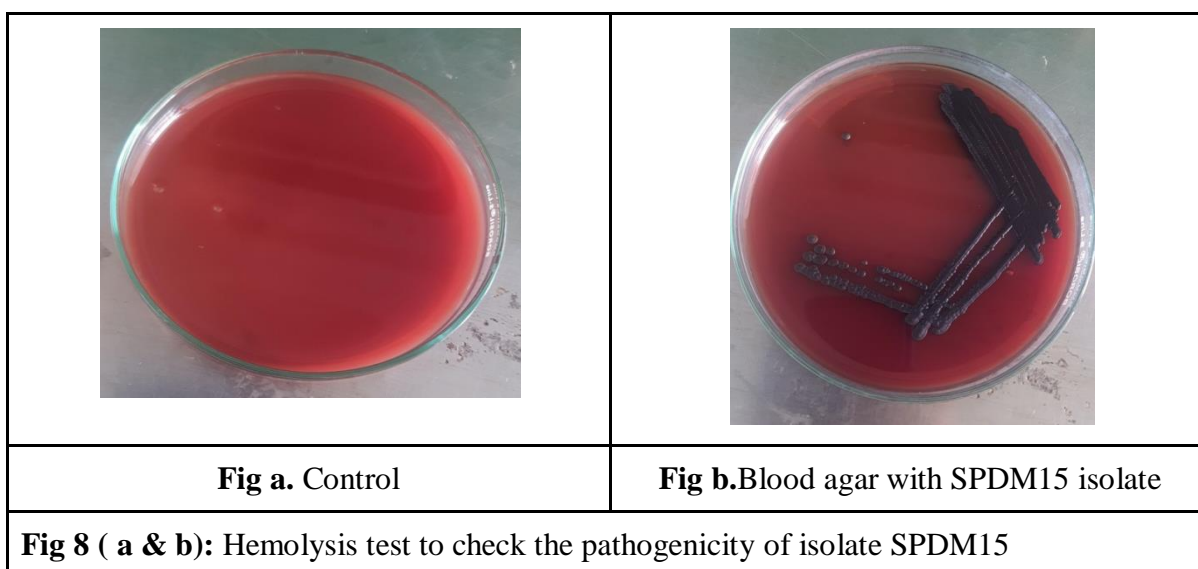
Fig7: Phylogenetic tree of SPDM15 species and related taxa, based on the ITS region

The phylogenetic tree shows the relation of SPDM15 with *Hortaea werneckii*, the overlaps indicate that they show high similarity. The outgroup used was *Saccharomyces cerevisiae*.

4.5 Investigating the pathogenicity of isolate SPDM15:

4.5.1 Hemolysis test

A hemolysis test was conducted on the SPDM15 culture to assess its potential to lyse red blood cells (RBCs), thereby aiding in the determination of its pathogenicity. Hemolysis test to check the pathogenicity of isolate SPDM15 is depicted in **Fig 8 (a & b)**, where fig a represents the control plate and fig b shows the blood agar plate streaked with isolate SPDM15.



The yeast isolate showed Gamma hemolysis (γ) on the blood agar medium that indicating the lack of hemolysis. Since it showed no reaction in the surrounding medium.

Beta hemolysis (β), characterized by complete or true lysis of red blood cells, manifests as a clear zone surrounding the colony, approaching the color and transparency of the base medium. On the other hand, Alpha hemolysis (α) involves the reduction of red blood cell hemoglobin to methemoglobin in the medium surrounding the colony, resulting in a green or brown discoloration. However, no evidence of Alpha and Beta hemolysis was observed in this case.

4.6 Screening of bioactive molecules from SPDM15 and its application

Bioactive molecules which are formed as a result of microbial activity can have diverse pharmacological activities and applications hence screening for it could have a great potential for treatment of wastewater, diseases etc

4.6.1. Extraction, partial identification and antimicrobial activity of pigment from isolate SPDM15

A) Extraction of pigment from SPDM15

As seen the isolate SPDM15 showed black pigmentation hence pigment extraction procedures were undertaken for further analysis. The pigment was extracted from SPDM15 after growing in 10% NTYE media as depicted in **Fig 9**



Fig 9: Pigment extracted from SPDM15 after growing in NTYE media.

Pigment was extracted after inoculating the culture in 10% salt concentration NTYE media. NaOH was used to lysed the yeast cell. Since the pigment was soluble in NaOH it dissolved in it. Later HCl was used to precipitate this pigment and the pigment was extracted, a dark black or brown powder was obtained. From 50ml broth ,28 mg of pigment was obtained. The pigment was insoluble in water and soluble in NaOH and DMSO.

In the investigation, *Hortaea werneckii*, a black yeast, was found to produce 5.60g/L of melanin pigment under optimized conditions. Glucose emerged as the most favorable carbon source for melanin production in comparison to alternative sources. This finding mirrors previous observations where glucose was identified as the optimal carbon source, resulting in a high melanin yield (7.22g/L) in *Yarrowia lipolytica*. Conversely, starch demonstrated effectiveness as a carbon source for *Streptomyces* sp., followed by glycerol and fructose. Regarding nitrogen sources, peptone induced hyper secretion of pigment relative to yeast extract and corn steep, consistent with prior reports. Combining yeast extract and peptone in a single medium proved beneficial for enhancing pigment production. Rice bran exhibited notable efficacy among substrates, yielding a high quantity of pigment. The highest pigment production was attained at 30°C, pH 7.0, and salinity of 15%, with the optimum pH and temperature recorded at pH 7.0 and 32°C, respectively. *Aspergillus carbonicus* synthesized the maximum amount (20.76g/L) of pigments during the 15th to 25th day of the incubation period. (Kalaiselvam et al., 2013)

B) FTIR analysis of pigment

Isolate SPDM15 produces dark brown or black pigment. FTIR analysis was done in order to partially identify the pigment. The pigment showed similar functional groups present in melanin pigment and it was confirmed by comparing it with a standard FTIR spectra. Fig 10 depicts the Infra-red spectrum (FT-IR) of melanin pigment extracted from SPDM15 at 10% salt concentration in NTYE media. Standard FTIR spectra of melanin is shown in Fig 11.

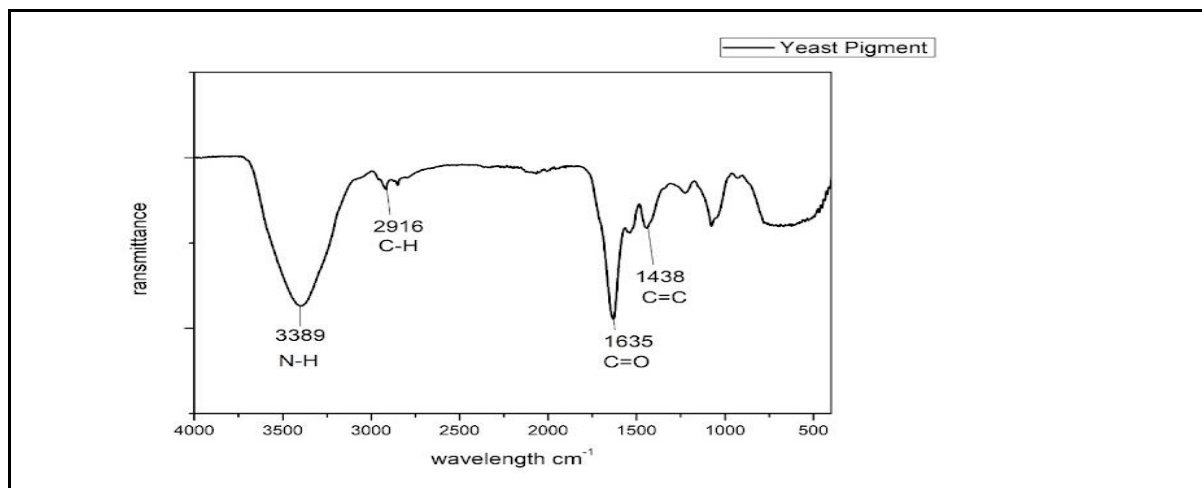


Fig 10 : Infra-red spectrum (FT-IR) of melanin pigment of SPDM15 at 10% salt concentration

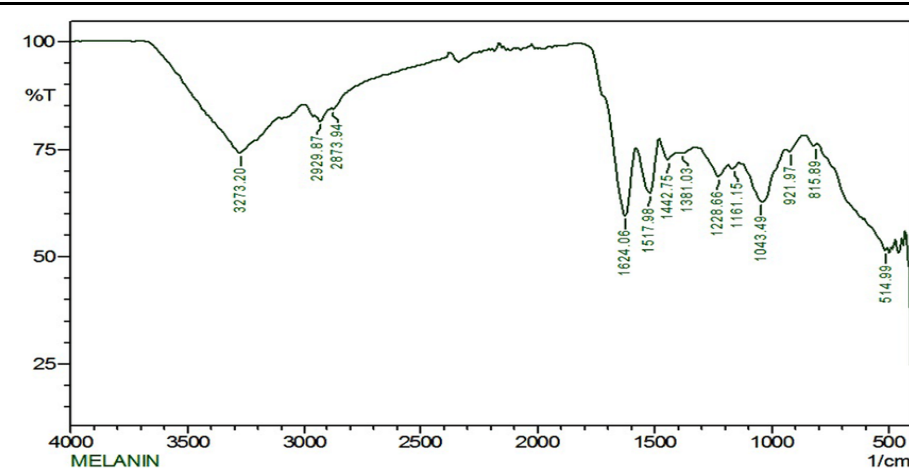


Fig 11: Standard FTIR spectra of melanin (Kiran et al., 2015)

Pigment absorbed at various wavelengths shows the specific functional groups present in the melanin, indicating that isolate SPDM15 produces melanin structure. There were significant peaks at 3389 cm⁻¹, 2916 cm⁻¹, 1635 cm⁻¹ and 1438 cm⁻¹ in FTIR spectra. 3389 cm⁻¹ peak shows the presence of the (N-H) amine group, 2916 cm⁻¹ (C-H) alkane group, 1635 cm⁻¹ (C=O) carbonyl group and 1438 cm⁻¹ (C=C) aromatic.

Melanin pigment consists of the amine, alkane, alkene, and carbonyl groups. This confirms the presence of melanin pigment. There were peaks present in the spectra showing the wavenumber between the 3350 cm⁻¹ to 3500 cm⁻¹ indicating N-H stretch and 2850 cm⁻¹ -2950

cm⁻¹ show C-H group. Also, from 1500 cm⁻¹ to 1700 cm⁻¹ is the C=O group. From 1400 cm⁻¹ to 1600 cm⁻¹ peaks observed show the presence of C=C aromatic group.

Previous studies have shown that IR spectra of melanin revealed peaks near 3,435 cm⁻¹, which were attributed to the amino second group (NH). The peak at 2,931cm⁻¹ was attributed to the methane group-related C-H stretch bond. NH₂ stretching caused the amino group to peak at 1,633 cm⁻¹. The anhydride group (C-O) in synthetic melanin and all extracted fungi pigment accounts for the peak at 1,267 cm⁻¹. This anomaly may be strain-related, or the C/N ratio may have been caused by contaminants that were challenging to remove from melanin (Soundra et al., 2013).

Some studies also show the pigment produced from *H. werneckii* ASI had significant peaks in its acquired FTIR spectra near 3438.31cm⁻¹, 2927.31 cm⁻¹, 1637.53 cm⁻¹, and 1239.90 cm⁻¹. The outcome was evaluated against a melanin standard acquired from Sigma Aldrich. The peak at 2927 cm⁻¹, which also suggests the presence of a significant number of aliphatic groups in the examined melanin structure, is the most obvious difference between the synthetic melanin standard and the *H. werneckii* AS1 pigment (Elsayis et al., 2022).

The peaks absorbance was confirmed by comparing the data with Libretexts ([https://chem.libretexts.org/Ancillary Materials/Reference/Reference Tables/Spectroscopic Reference Tables/Infrared Spectroscopy Absorption Table](https://chem.libretexts.org/Ancillary_Materials/Reference/Reference_Tables/Spectroscopic_Reference_Tables/Infrared_Spectroscopy_Absorption_Table)).

4.6.2Dyeing of cotton fabrics using melanin pigment.

Utilising pigment extracted from yeast can help in the eco-friendly dyeing of fabrics. Cotton fabric was used to dye it with melanin pigment. Figure 12 (A to C) illustrates the dyeing process of cotton fabric using melanin pigment derived from the SPDM15 isolate. Fig. A, B and C represent the Synthetic, Natural and combination of mordants used as a fixative agent to the dye on cotton fabric, respectively. In Figure A, the sub-figures a, b, and c denote the application of Potassium dichromate, Ferrous sulphate, and Cupric sulphate as mordants on

the fabric prior to dyeing, respectively. In Figure B, sub-figures a, b, and c represent the use of alum, aloe vera, and lemon as mordants for the cloth before dyeing, respectively. Figure C displays the application of various combinations of mordants on cotton fabric prior to dyeing, with sub-figures a, b, and c showing Alum + sodium carbonate, Ferrous sulphate + alum, Aloe vera + alum, and lemon + alum as mordant combinations, respectively.

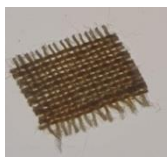
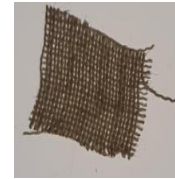
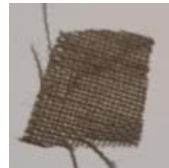
Before dyeing	After dyeing	After washing	After wet rubbing	Light exposure
Fig A. Synthetic mordants				
				
a. Potassium dichromate as mordant				
				
b. Ferrous sulphate as mordant				
				
c. Cupric sulphate as mordant				

Fig B. Natural mordants

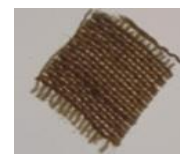
a. Alum as mordant



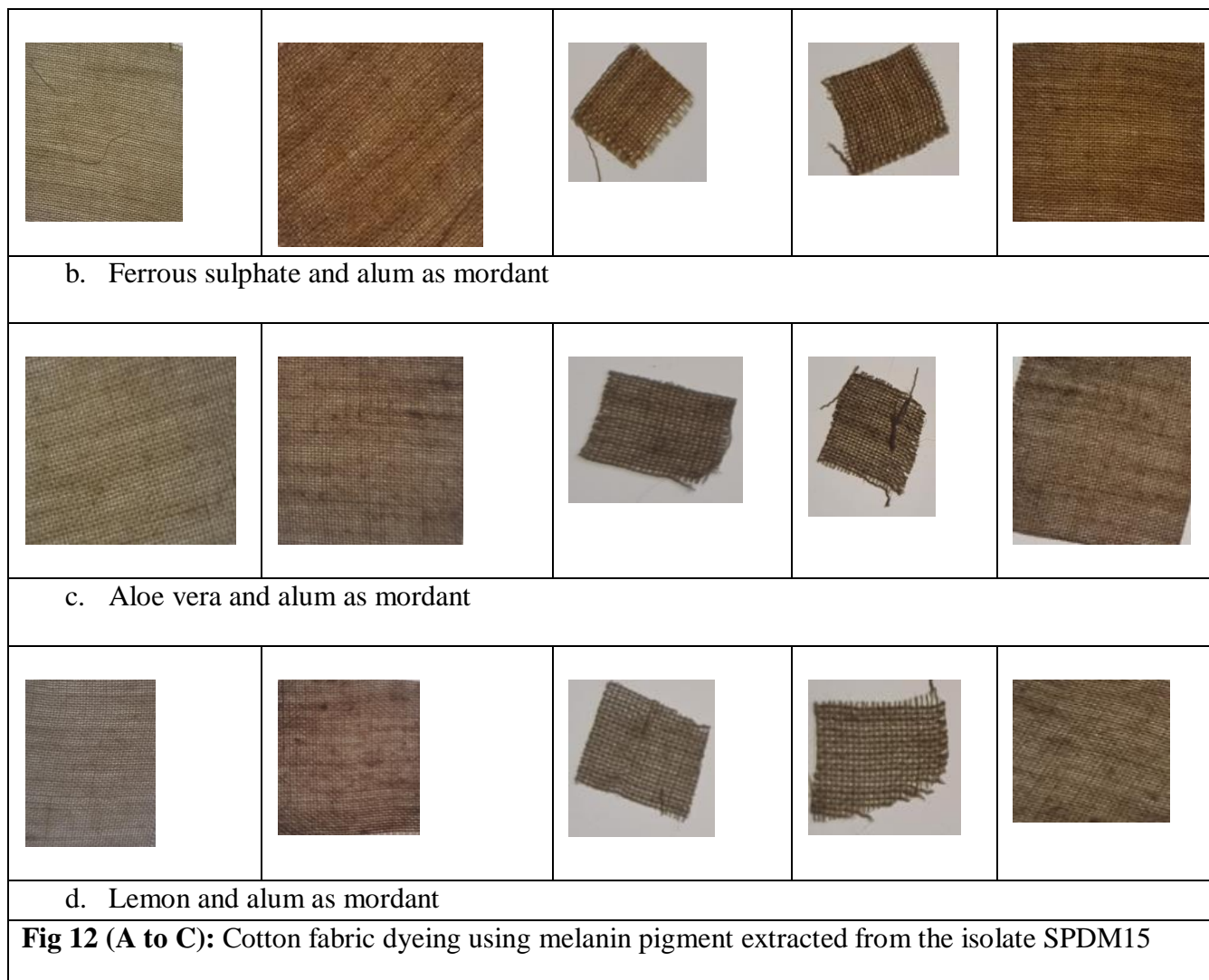
b. Aloe vera as mordant



c. Lemon as mordant

Fig C. Combinations of mordants

a. Alum and sodium carbonate as mordant

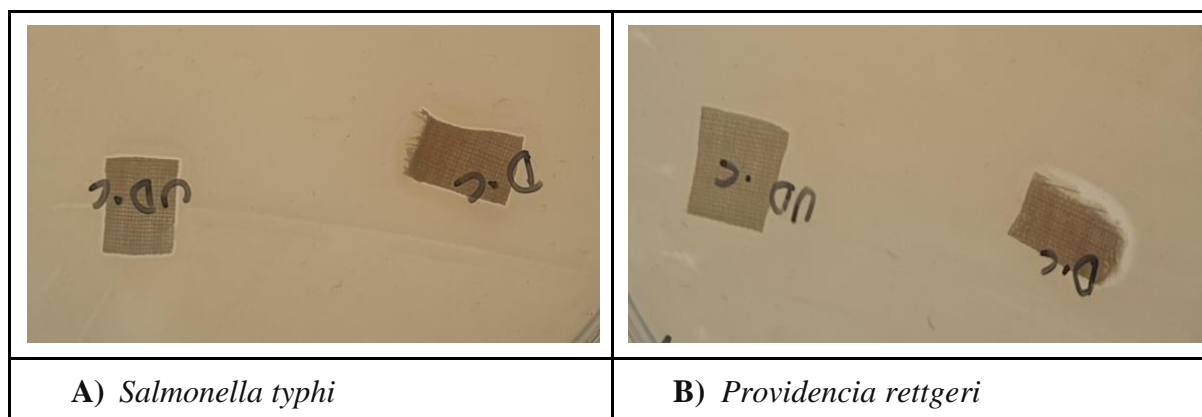


For the dyeing experiment, cotton fabric was used. Initially, the cloth underwent a thorough cleansing process involving sodium lauryl sulfate and HCl treatment to eliminate any impurities. Prior to dye application, pre-mordanting occurred using various types of mordants (natural, synthetic, and combinations of different mordants), which act as binding agents that facilitate the adherence of natural dyes to the fibres. During the dyeing stage, sodium sulfate anhydrous was combined with the pigment to ensure the uniform distribution of dyes onto the fabric fibres. This process enhances dye dispersion, producing vibrant and consistent colours, yielding high-quality dyed and printed textiles. Additionally, post-mordanting was carried out to further enhance colour fixation and improve the durability of dyes on the textile fibres. The cotton fabric treated with mordants alum and sodium carbonate developed a medium dark

shade of red-orange and exhibited better pigment absorption and binding properties. Even after washing, wet rubbing, and exposure to sunlight, only a slight shade difference was observed, with shade change to a medium dark shade after exposure to sunlight. After washing and wet rubbing, the colour changed to a medium-dark shade of orange and brown, respectively. Similarly, when ferrous sulphate and alum were employed as mordants for cotton fabric, they gave a pale brown colour with notable pigment absorption compared to other mordants. After washing, wet rubbing, and exposure to sunlight, the colour changed to light brown, saddle and dark tan shade. Thus, indicating that the combination of natural and synthetic mordants enhances color absorption more effectively. However, the use of natural mordants resulted in uneven dyeing of the fabric and subsequent colour fading after washing and wet rubbing. Mordants such as potassium dichromate, ferrous sulphate, and cupric sulphate also yielded unsatisfactory results with inadequate dyeing of the cotton fabric.

A. Qualitative analysis of antibacterial properties of dyed cloth:-

The evaluation of antibacterial was carried out since fabric dyed with pigment having antibacterial activity could be used to clothes for hospitals have antibacterial properties. **Fig 13(A to C)** depicts the Antibacterial properties of dyed cloth with mordant Alum + Sodium carbonate. Figures A, B, and C show the antibacterial activity of dyed cloth against *Salmonella typhi*, *Providencia rettgeri* and *Klebsiella pneumonia*, respectively. UD.C and D.C represent undyed cloth and Dyed cloth, respectively.





C) *Klebsiella pneumoniae*

Fig 13(A to C) :Antibacterial property of dyed cloth with mordant Alum + Sodium carbonate

Antibacterial activity was found positive against *Salmonella typhi*, *Providencia rettgeri* and *Klebsiella pneumonia* with cotton fabric dyed with melanin pigment and treated with mordants, alum and sodium carbonate as shown in fig 13.

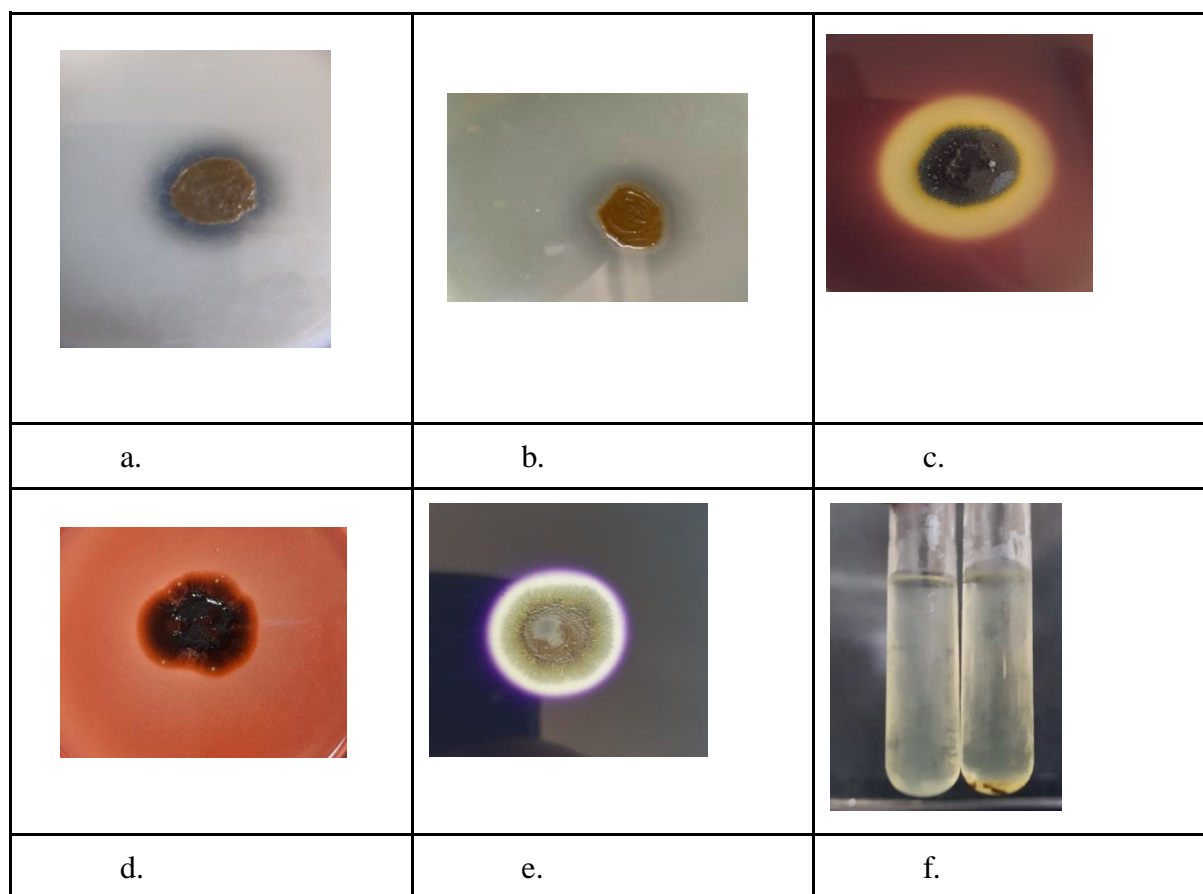
Researchers have found that melanin can effectively combat several bacterial strains. For instance, it has been shown to be effective against *Salmonella typhi*, *Vibrio parahaemolyticus*, and *Klebsiella pneumoniae* (Helan et al., 2013).. Additionally, melanin exhibits efficacy against bacteria such as *Escherichia coli*, *Lactobacillus vulgaris*, *Staphylococcus aureus*, *Proteus mirabilis*, *Vibrio cholera*, *Salmonella paratyphi*, and *Klebsiella oxytoca* (Kejžar et al., 2013),. Interestingly, it has no impact on the tested *Bacillus subtilis*, *L. monocytogens*, *S. pneumoniae*, *K. pneumoniae*, and *P. aeruginosa* strains (Hodhod et al., 2020). These findings underscore the potential of melanin as a natural antimicrobial agent, offering broad-spectrum protection against various bacteria.

In a study, the antibacterial properties of treated fabrics were assessed against common pathogenic bacteria, namely *Staphylococcus aureus* (Gram-positive) and *Escherichia coli* (Gram-negative). The effects of dye concentration and mordant types on the resulting color tones, antibacterial effectiveness, and color retention of the fabrics were examined. The findings revealed that fabrics treated with mordants and dyes exhibited favorable antibacterial properties. Complete antibacterial efficacy of the treated fabrics was achieved with 3% owf

(on weight of the fabric) copper sulfate. Additionally, it was demonstrated that increasing the dye concentration could enhance the antibacterial effectiveness on mordanted dyed fabrics. An optimal level of antibacterial activity was observed in the sample treated with 30% owf of turmeric. (Ghoreishian et al., 2013)

4.6.3 Screening of SPDM15 isolate for Enzyme involved in plant polymer degradation:

The isolate was screened for the production of plant polymer degrading enzymes. Extracellular enzyme production is depicted in **Fig 14(a to m)**, the subfigures a, b, c, d, e f, g, h, i, j, k, l and m represent protease, xylanase, pectinase, cellulase, amylase, gelatinase, urease, catalase, esterase, laccase, agarase, lipase and chitinase activity respectively.



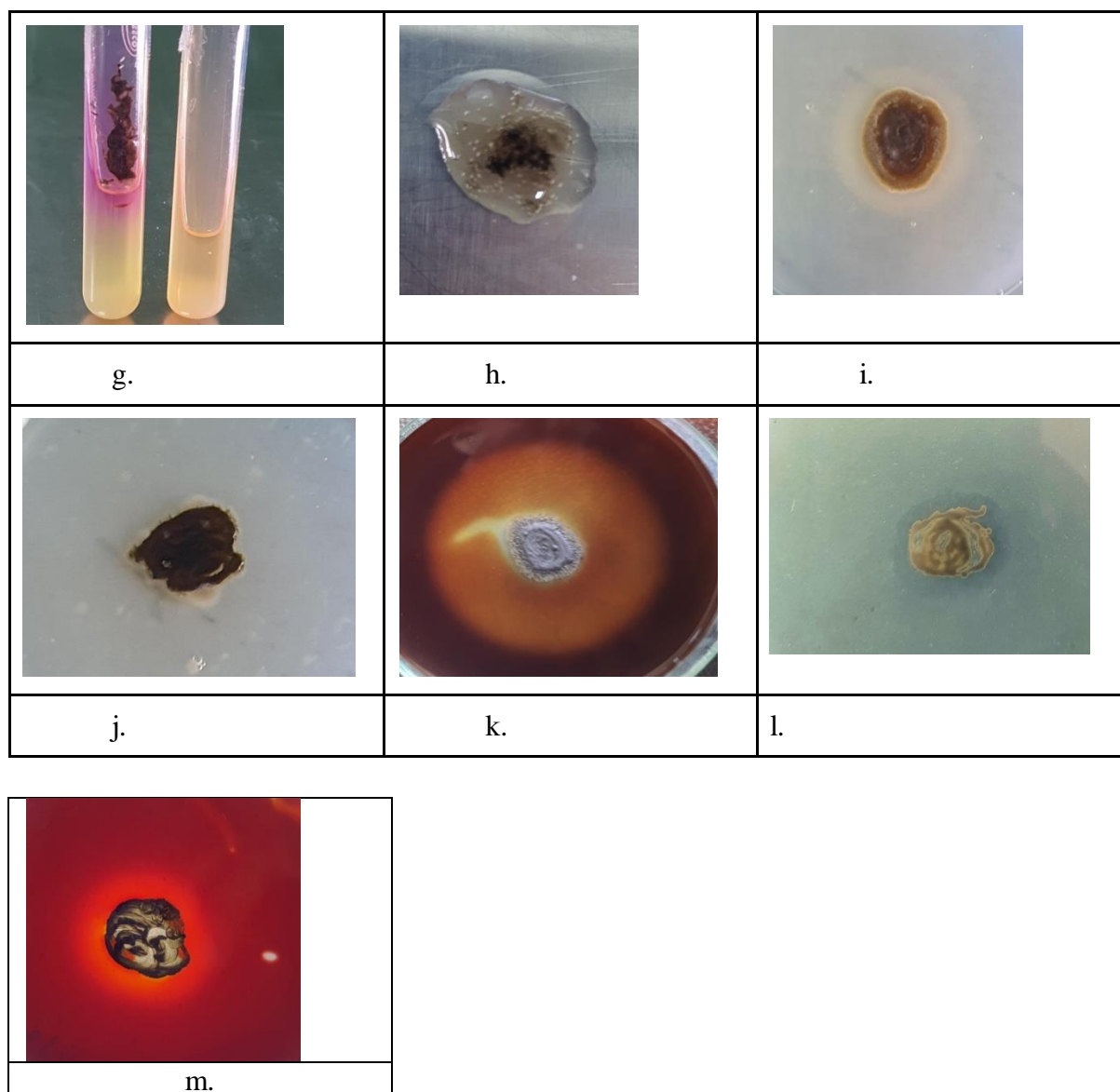


Fig 14 (a to m) : Extracellular enzyme production test. a) protease. b) xylanase. c) pectinase. d) cellulase. e) amylase. f) gelatinase. g) urease. h) catalase. i) esterase. j) laccase. k) agarase. l) lipase m) Chitinase

In the investigation, isolate SPDM15 was found to exhibit enzymatic activities, including amylase, xylanase, pectinase, cellulase, lipase, esterase, and agarase, as shown in Fig 14. The presence of these enzymes was observed through distinct clearance zones on their respective media. Additionally, urease activity was detected by a noticeable change in colour from light

orange to pink, which was due to the breakdown of urea by the isolate, leading to the production of ammonia, causing an increase in pH. The increase in pH causes the colour change of phenol red from light orange to pink. Meanwhile, catalase activity was evidenced by the presence of effervescence since the enzyme detoxified hydrogen peroxide by breaking it down into water and oxygen gas. The bubbles are due to the production of oxygen. No detectable levels of laccase and gelatinase enzymes were observed.

It has been seen that four strains of *Hortaea werneckii* from Brazil produce plant-targeting enzymes, including amylase, lipase, esterase, pectinase, and cellulase. These strains do not express animal-associated enzymes like albuminase, keratinase, phospholipase, or DNase. Urease production was consistent, while caseinase, gelatinase, and laccase varied among the strains .(Formoso et al., 2015)

4.6.4 Exopolysaccharide Screening Test:

To assess the extracellular polymeric substance (EPS) production by yeast, the organism was streaked onto Congo red agar plates. **Fig 15** depicts the exopolysaccharide production by the isolate SPDM15.

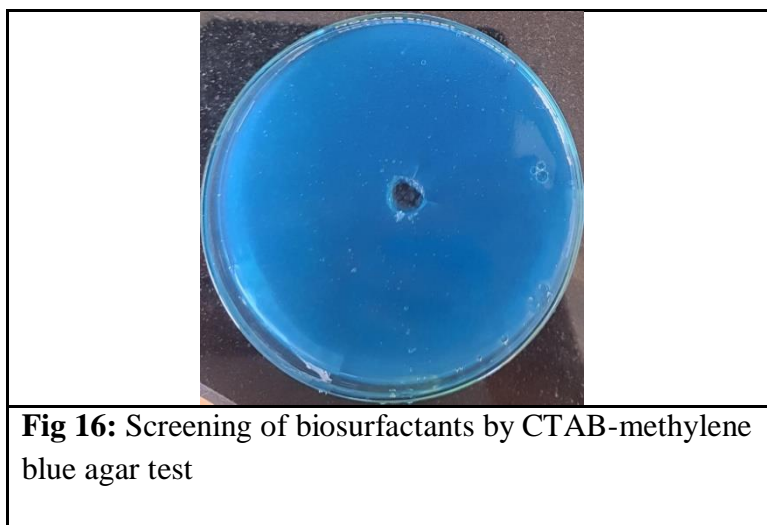


Fig 15: Yeast isolate screened for EPS production

The yeast isolate screened for EPS production gave positive results as intense black colouration. Extracellular polysaccharides are produced by many species of yeast, such as strains of *Bullera*, *Candida*, *Cryptococcus*, *Debaryomyces*, *Lipomyces*, *Pichia*, *Pseudozyma*, *Rhodotorula* and *Sporobolomyces* genera (Gientka et al., 2015)

4.6.5 Screening for Biosurfactant Production:

To assess the yeast's potential to produce surface-active compounds, namely biosurfactants, the CTAB methylene blue agar test was performed. **Fig 16** illustrates the screening of biosurfactants from isolate SPDM15 using this test.



The yeast isolate screened for biosurfactant production gave negative results since there was no dark blue halo and a yellow zone of clearance around the colony.

In a study, nine morphologically distinct halophilic yeasts were isolated from Makgadikgadi and Sua pans, extreme environments in Botswana. Screening for biosurfactant production revealed that *Rhodotorulamucilaginoso SP6* and *Debaryomyceshansenii MK9* exhibited the highest biosurfactant activity using Xanthocerciszambesiaca seed powder as a novel and cost-effective alternative carbon substrate. These two biosurfactants exhibited antimicrobial

activities against eight pathogenic bacteria and fungal strains (*Proteus vulgaris*, *Escherichia coli*, *Klebsiella pneumoniae*, *Staphylococcus aureus*, *Micrococcus luteus*, *Cryptococcus neoformans*, *Candida albicans*, and *Aspergillus niger*). (Loeto et al., 2021)

4.7 Accelerating composting process with inoculation of SPDM15 culture:

The isolate SPDM15 produced a wide no of plant polymer degrading enzymes. Hence, it could be used to fasten the decomposition of waste, aiding in accelerating the composting process, which can be sustainable and economical.

4.7.1 Analysis of Compost for various parameters

A) pH analysis

Determination of pH is vital to understand at which stage the compost is undergoing which can be understood by the change of pH in different time intervals. **Table 5** depicts pH analysis of compost sets.

Table 5: pH analysis of compost sets on day 0, 10 and 25.			
Compost set	pH on day 0	pH on day 10	pH on day 25
T1	6.42	7.08	8.34
T2	5.44	6.455	8.265
T3	5.07	6.79	8.065
T4	4.685	7.17	8.085
T5	5.4	7.115	7.855
T6	5.71	7.375	7.74

Fig 17 illustrates a graphical representation derived from the data presented in Table 5, which outlines the pH analysis of compost on days 0, 10, and 25.

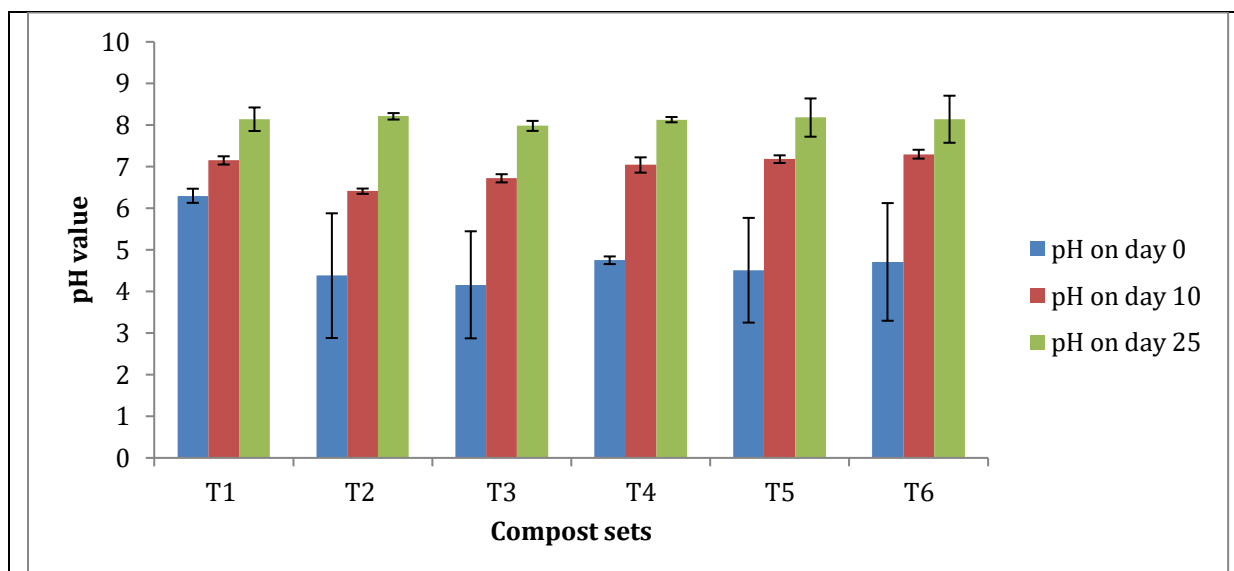


Fig 17: pH analysis of compost sets on day 0, 10 and 25.

Initially on the day 1 the pH was found to be acidic in all sets due to the release of organic acids during the decomposition of waste. After 10 days the pH was neutral except in set 2 and 3. On day 25 the pH in all compost sets was observed as alkaline.

According to De Bertoldi et al. (1983), organic material can be composted in a broad pH range (3–11). Optimal values are between 5.5 and 8. Values around neutrality are optimal for microorganisms' development. However, fungi are more tolerant to distant neutral pH than bacteria. The pH may decrease in the first stage of composting, due to the organic acids releasing during the decomposition of simple organic substrates, and volatilization of the initial ammonia. Thereafter, the disappearance of easily degradable organic materials and mineralization leading to an increase in pH (McKinley and Vestal 1985). At the end of composting, it is also possible to end in an acidic pH due to H^+ ions released during nitrification (Fang and Wong 1999). In reality, the changes in the pH depend significantly on the raw materials and any additive components of the initial mixture, as reported by Eklind and Kirchmann (2000) in the case of compost made from waste wood and paper. It also depends on the conditions of airflow of composting, for effective ventilation, for example,

allowing a good degradation of the organic material and resulting in a higher final pH (Ferrer 2001). Temperature also plays a role in the evolution of pH, favouring ammonia volatilization. The pH changes several times during composting. Generally, there are four phases (Poincelot 1972). In the Acid-genesis Phase (Phase I), there's a pH decline accompanied by significant CO₂ and organic acid production by the flora, occurring early in the thermophilic phase. The Alkalization Phase (Phase II) ensues, characterized by pH elevation. Bacterial hydrolysis of protein and organic nitrogen yields ammonia during this phase. Subsequently, in the pH stabilization phase (Phase III), the C/N ratio diminishes, leading to decelerated reactions. Ammonia volatilization, particularly evident with a pH surpassing 8, occurs while nitrogen serves as a substrate for microbial synthesis of new humic compounds. Finally, in the Stable Phase (Phase IV), the compost nears a neutral pH, marking its maturation. This phase's stability is attributed to sluggish reactions and the influence of humus as a buffer.

B) Total solid, volatile solid, Ash, and moisture content analysis

Determination of Total solid, volatile solid, Ash, and moisture content helps to understand the various properties of compost. Analysis of compost of day 1 for various parameters such as moisture, TS, Ash, VS for all the different sets of compost is depicted in **Table 6**.

Table 6: Analysis of compost of day 1 for various parameters such as moisture, TS, Ash, VS for all the different sets of compost .				
Compost sets	Moisture (%)	TS (%)	Ash (%)	VS (%)
T1	55.2	44.80	7.05	37.76
T2	51.89	48.11	4.36	43.74
T3	46.51	53.49	2.28	51.21
T4	74.35	25.65	3.28	36.02
T5	43.77	56.23	7.82	48.41
T6	45.88	54.12	9.29	44.82

Fig 18 depicts the graphical visualization derived from the data provided in Table 6, which details the analysis of compost on day 1 for various parameters including pH, moisture content, total solids (TS), volatile solids (VS), and ash content.

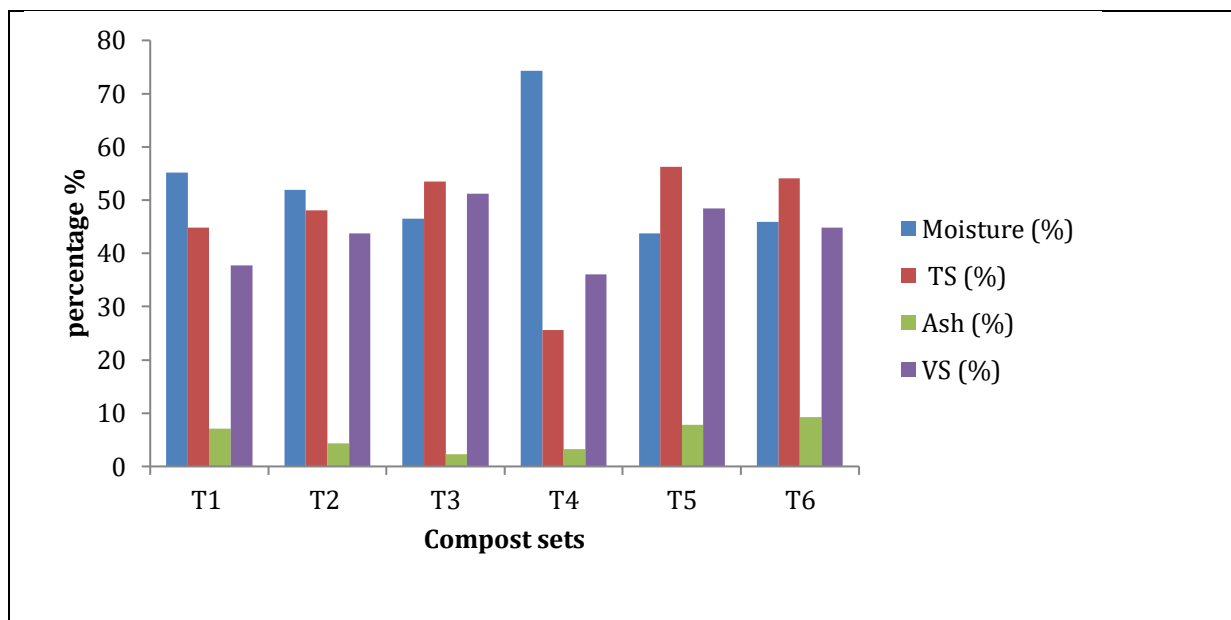


Fig 18 : Compost of day 1 analysed for various parameters such as pH, moisture, TS, VS, Ash.

In order to achieve efficient compost formation, it is crucial to regulate moisture. Hence, various parameters including moisture content, total solids (TS), ash content, and volatile solids (VS) were analysed. The optimal moisture range is between 45% and 60%. When moisture is less than 30%, the bacterial activities will be limited and that above 65% will decrease the porosity of the compost resulting in an anaerobic growth and unpleasant odour emission. (Razmjoo et al. 2015) The moisture content fell within the optimum range for all sets except for set 5, which required additional maintenance through water sprinkling to attain the desired level. No foul odour production was observed. VS help us to determine whether the substance is biodegradable or not. Volatile solids found in T1, T2, T3, T4, T5 and T6 were 37.76%, 43.74%, 51.21%, 36.02%, 48.41% and 44.82% respectively. More biodegradable substances were present in T3 followed by T5, T6, T2, T4, T1. The ash

content in biomass refers to the inorganic residues that remain after combustion at a temperature of 575°C. These inorganic materials typically include minerals such as silica, calcium, potassium, iron, sodium, magnesium, aluminum, and titanium. Essentially, it represents the non-combustible fraction of biomass, which can have implications for various processes, including energy production and environmental impact (Shadangi et al., 2015). The ash content in T1, T2, T3, T4, T5 and T6 was found to be 7.05%, 4.36%, 2.28%, 3.28%, 7.82% and 9.29% respectively. T6 has highest inorganic residues followed by T5, T1, T2, T4 and T3.

Achieving optimal moisture levels during composting, especially in open environments, can be challenging. In practice, this challenge is often addressed by monitoring temperature, which serves as an indicator for determining the appropriate timing for turning, moistening, and ventilating the compost pile (Tiquia and Tam, 1998). Insufficient initial moisture levels, typically below 30%, can result in rapid compost dehydration, halting biological processes and yielding physically stable but biologically inactive compost (De Bertoldi et al., 1983). Conversely, excessive moisture levels, exceeding 80%, can create anaerobic conditions within the compost. Therefore, it is crucial to identify the optimal moisture range for the composting process (Yulipriyanto, 2001). Razmjoo et al. (2015) observed that moisture levels ranging between 45% and 50% are optimal for composting. Moisture levels below 30% limit bacterial activity, while levels above 65% reduce compost porosity, leading to anaerobic conditions and unpleasant odors. Monitoring of moisture content in windrows revealed a typical trend, with levels starting at 46% to 51% in the first month and decreasing to 42% to 47% by the end of the third month of operation. The moisture content of the first windrow was initially lower due to higher paper content in its raw materials. However, manual water spraying on the first windrow during the third month increased its humidity. Overall, the observed humidity ranges were deemed ideal for the composting process in the study.

C) Temperature analysis of compost

It is essential to monitor the temperature as it can help to determine at which stage the compost is at and also the maturity of the compost. **Table 7** shows the data of temperature for all sets for 20 days.

Days	T1	T2	T3	T4	T5	T6
1	38.5	47	44	38	38	42
2	46	50	44	49	47	50
3	43.5	36	36	36	31	33
4	48	48	48	47	49	46
5	45.5	51	52	51	49	49
6	44	50	53	43	44	47
7	45	52	46	46	45	48
8	41	43	44	38	41	40
9	41	40	40	38	38	38
10	40.5	37	39	37	37	37
11	41	39	40	37	38	38
12	37.5	34	35	35	34	33
13	34	33	32	32	30	30
14	33	34	34	34	34	35
15	32	30	33	31	31	31
16	36.5	35	37	35	39	35
17	33	36	34	33	33	32
18	34.5	36	37	36	36	36
19	35	35	35	35	36	35
20	34.5	35	35	34	34	35

Fig 19 depicts the graphical representation of data from Table 7 showing temperature monitored for 20 days of different compost sets.

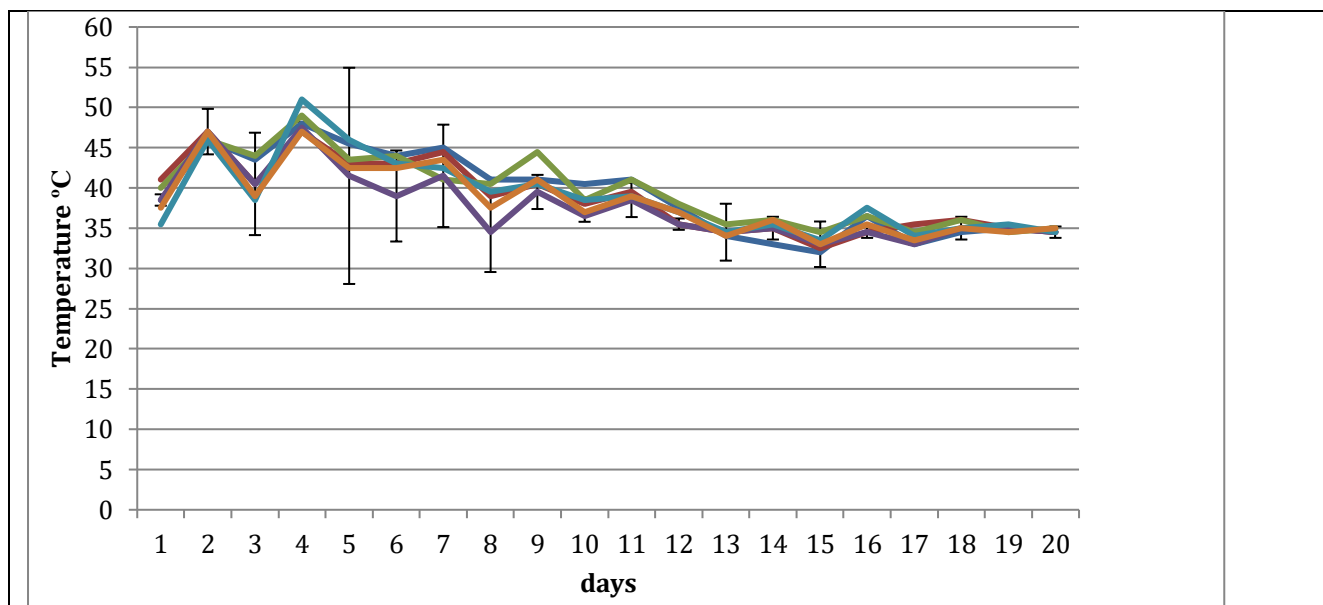


Fig 19 : Temperature monitored for 25 days of different compost sets

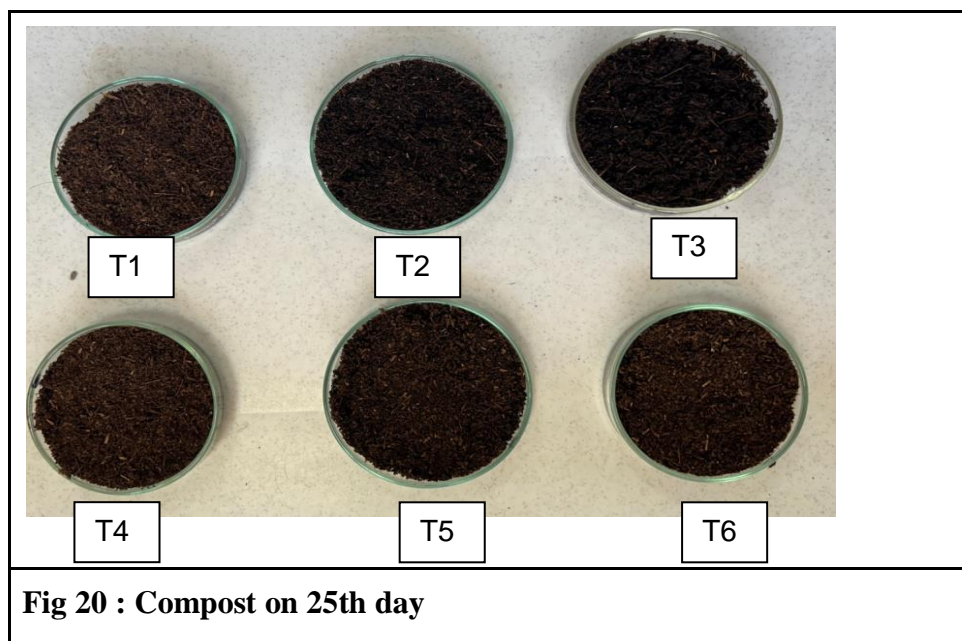
Monitoring temperature is crucial for assessing the composting process. It helps identify the different phases, such as mesophilic, thermophilic, and cooling. Initially, the temperature ranged from 30°C to 48°C across all sets for three days except T2, T4 and T6 in which the temperature was high. During this time, the mesophilic phase occurred, characterized by increasing temperatures due to the biodegradation of organic compounds by mesophilic microorganisms. On the fourth day, the temperature rose to around 50°C, signaling the start of the thermophilic phase. In this phase, thermophilic microorganisms replaced the mesophilic ones, breaking down soluble and readily degradable compounds. From the 12th day onward, the temperature decreased as the compost entered the cooling phase.

During the composting process, temperature variations occur predominantly in three distinct phases: mesophilic, thermophilic, and cooling phases. The mesophilic phase, observed within the initial days of composting, is characterized by a rise in temperature primarily due to the

biodegradation of organic compounds facilitated by increased proliferation of mesophilic microorganisms. Fourtiet al. documented a gradual temperature increase to the range of 25-45°C within 25 days of composting. Transitioning to the thermophilic phase, temperatures escalate beyond the tolerance limit of mesophilic microorganisms (>45°C). Fourti et al. noted temperature elevations predominantly surpassing 40°C within 30 to 130 days, attributing the rise to the predominance of thermophilic microorganisms replacing mesophiles. The onset of this phase is expedited in compost rich in easily degradable materials, as demonstrated by Ocana et al., who recorded a peak temperature of 70°C within 15-20 days post-initiation of composting. This phase's establishment is rapid, with minor temperature fluctuations possibly attributed to humidification, indicating the persistence of under-composed materials post-thermophilic phase.

In the cooling phase, as organic matter (OM) depletes, temperatures gradually decrease, and the Carbon-to-Nitrogen (C/N) ratio stabilizes. Fourti et al. observed a rapid temperature decline to an average of 33°C by the 19th week, with no further temperature changes noted by the end of the fifth month despite interventions such as turning or water addition. The primary reason for temperature reduction during the cooling or maturity phase is the depletion of available substrate, leading to the replacement of thermophilic microflora by mesophiles. Partial degradation of recalcitrant compounds, predominantly cellulose and to a lesser extent lignin, persists under mesophilic microflora. Maturity is predominantly achieved upon reaching the cooling phase.

Fig 20 represents the compost of different sets after 25 days.



Dark brown black colour compost was seen in T3 and T2. Black colour compost was seen in T1, T4, T5 and T6. All the compost were soluble in water. The compost was of 25th day was then utilised for phytotoxicity analysis and CHNS analysis.

4.7.2 Phytotoxicity analysis of compost

This test is conducted to assess and monitor the potential toxicological impacts of different compost samples obtained post-composting. Phytotoxicity analysis of compost extract using Cowpea seeds (*Vigna unguiculata*) for Day 0 depicted in Fig 21 (A to J). In Fig A, B, C, D, E, F, G, H, I and J shows that the cowpea seeds were sprinkled with T1, T2, T3, T4, T5, T6, water, T7, soil and market compost extract respectively.

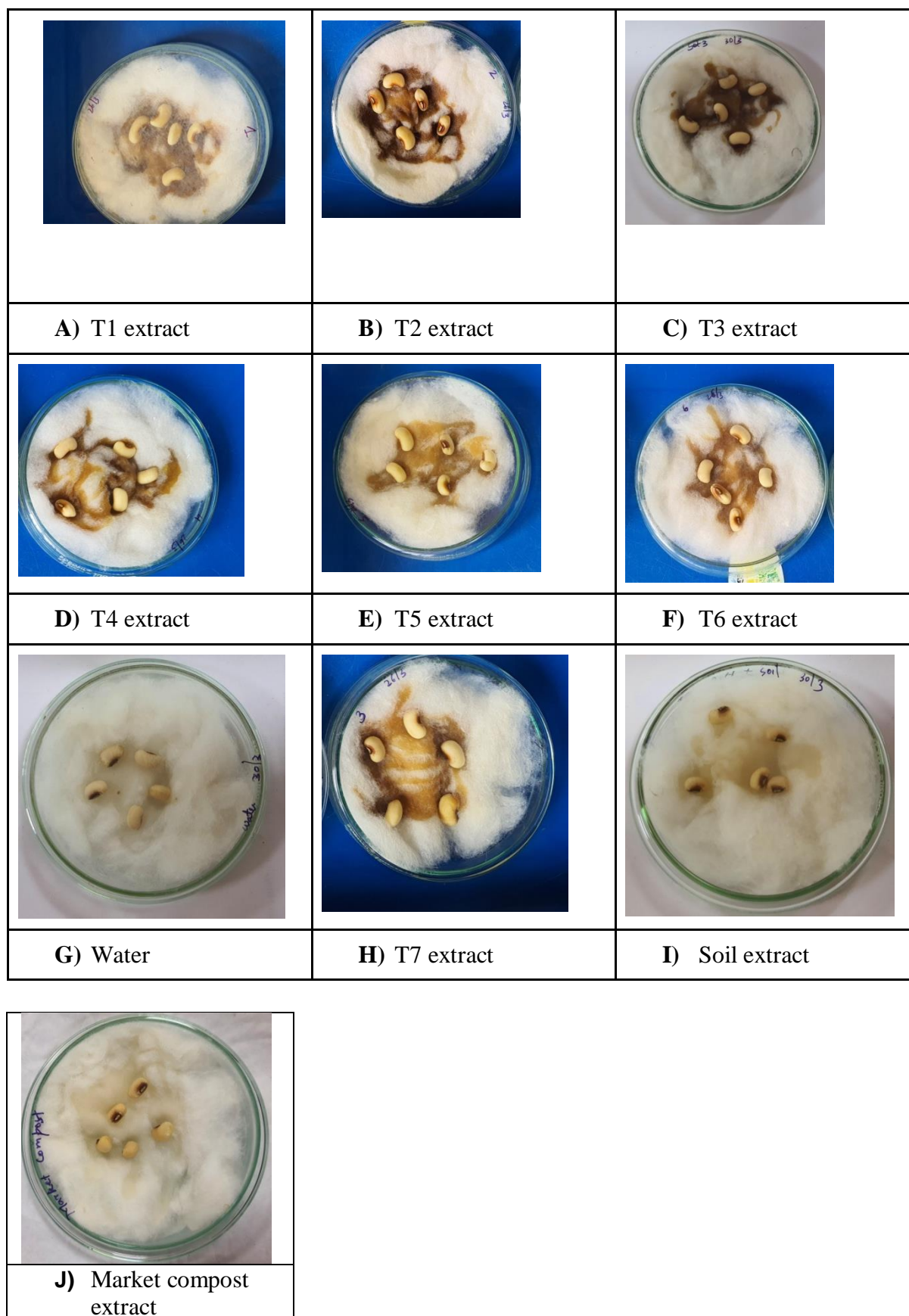
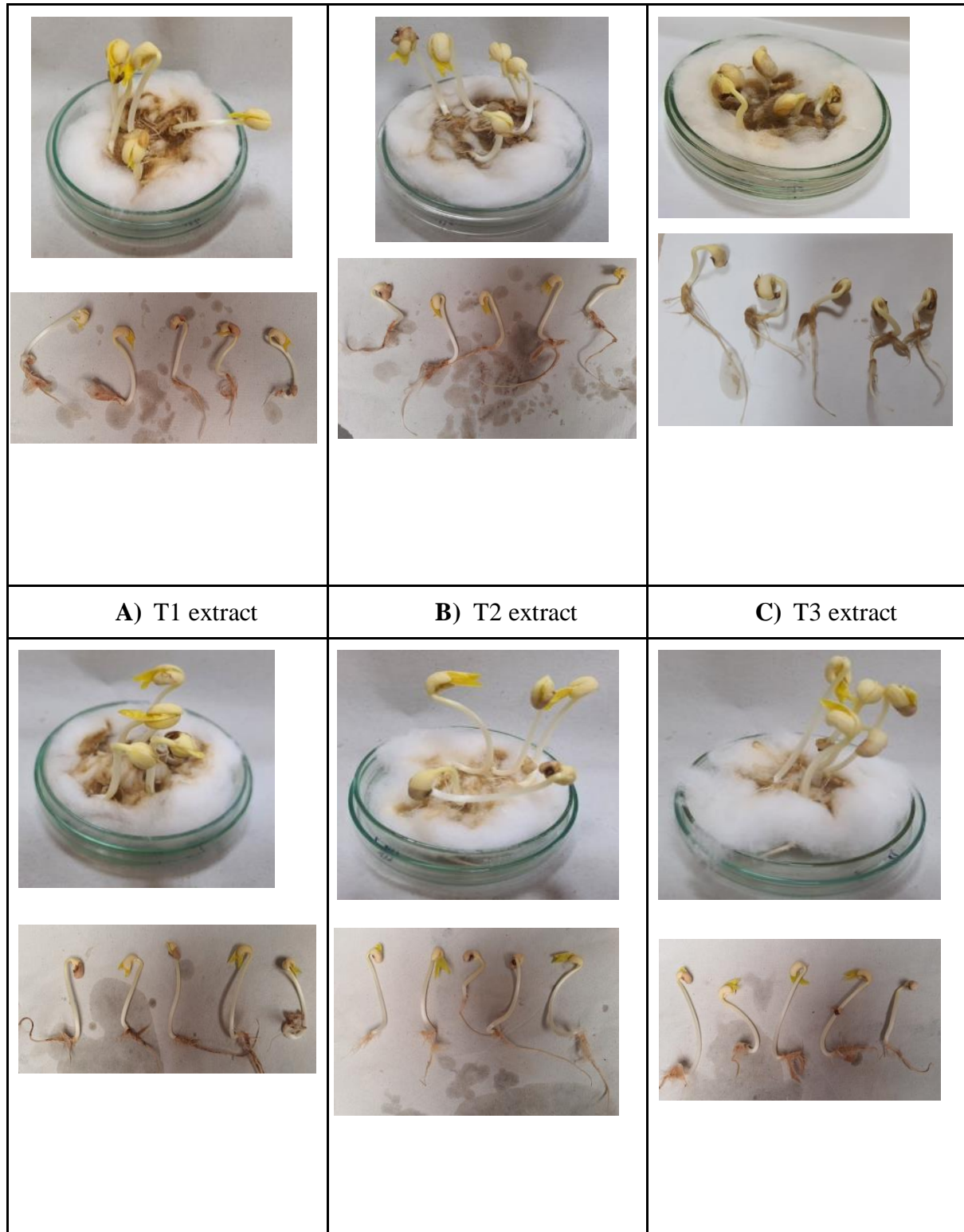
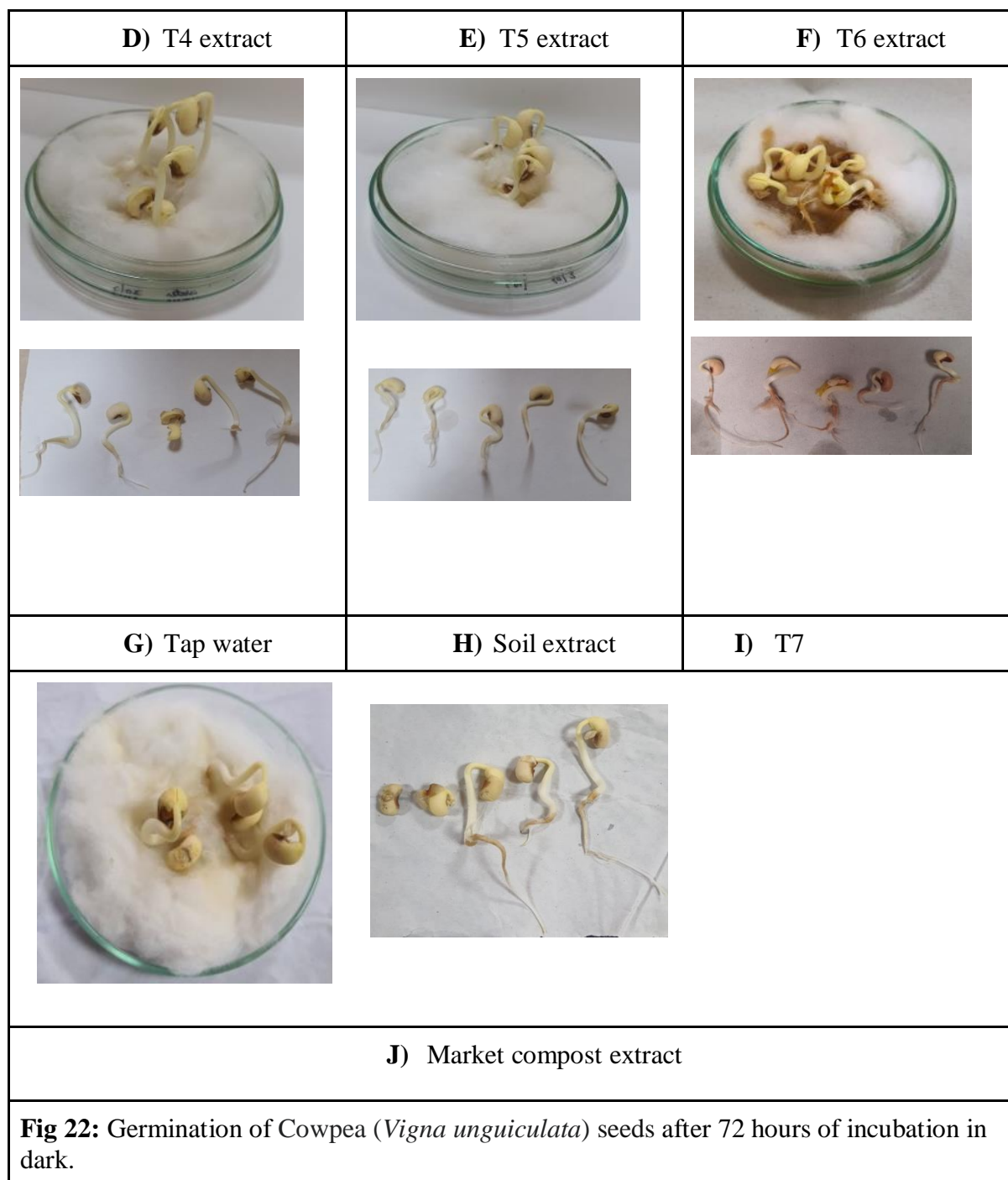


Fig 21 (A to J) :Phytotoxicity analysis of compost extract using Cowpea (*Vigna unguiculata*) seeds , Day 0

The **Figure 22** illustrates the inoculation of cowpea seeds in various extracts. Following inoculation, the seeds were subsequently incubated in darkness for 72 hours, aligning with the natural growth conditions of seeds in soil under absence of light.





After incubation in dark for 72 hrs, the total length was measured. The germinated seeds and non germinated seeds number was noted down to calculate the germination rate and vigor index.

It is essential to calculate the germination rate, which helps to estimate the viability of the population of seeds in the presence of compost extract. **Table 8 depicts** the determination of germination rate (%) and Vigor index to estimate the phytotoxicity of compost sets.

Table 8 : Determination of germination rate (%) and Vigor index to estimate the phytotoxicity of compost.					
Different sets	Total no of seeds	Total germinated seeds	Germination rate (%)	Average Total seedling length	Vigor index
T1	5	5	100	10.08	1008
T2	5	5	100	14.56	1456
T3	5	5	100	8.96	896
T4	5	5	100	14.46	1446
T5	5	5	100	13.84	1384
T6	5	5	100	12.38	1238
Tap water (control)	5	5	100	7.88	788
soil	5	5	100	6.78	678
T3 + yeast culture	5	5	100	10.46	1046
Market compost	5	4	80	8.54	683.2

The impact of compost extract on cowpea (*Vigna unguiculata*) seed germination was evident in terms of germination rate and vigor index after three days of incubation in the dark, compared to the control (tap water). The vigor index of T1, T2, T3, T4, T5 and T6 was found to be 1008, 1456, 896, 1446, 1384, 1238, 788, 678, 1046, 683.2. The seeds treated with T2 extract showed significant higher vigor index. The lowest vigor index was seen for soil of 678.

Mature compost is often utilized to enhance soil fertility and promote plant growth, as noted by Piccolo et al. (2004). However, the use of immature compost may hinder plant development due to oxygen competition within the rhizosphere and the release of potentially harmful substances, as highlighted by Bernal et al. (2009). Hence, conducting phytotoxicity analyses on compost is essential to evaluate its impact on seed germination and ensure its suitability for agricultural application.

Fungi from diverse classes and habitats, such as *Aspergillus*, *Fusarium*, *Penicillium*, *Piriformospora*, *Phoma*, and *Trichoderma*, are commonly reported as plant growth-promoting fungi (PGPF) (Devi et al. 2020; Ruppel et al. 2013). These fungi have been associated with improvements in germination, seedling vigor, biomass production, root hair development, photosynthetic efficiency, flowering, and yield. Some strains even enhance plant biochemical composition. While reports on halotolerant fungi with plant growth-promoting properties are limited, *Trichoderma* stands out as a versatile fungus that exhibits such traits even under salt stress conditions. (Oskiera et al. 2015; Poosapati et al. 2014). In a study, Hamayun et al. (2017) examined the *Porostereum* fungal species, which is known to produce phytohormones such as gibberellins, jasmonic acid, abscisic acid, and isoflavones. These phytohormones serve to mitigate salt stress and enhance the growth of soybean plants under salt stress conditions of less than 250 mM. Additionally, they explored the role of halotolerant mycorrhizal fungi like *Glomus* and *Xerocomus* in promoting the growth of various plant species including Acacia, Jatropha, ryegrass, and tea plants, as reported by Guo et al. (2022), Kumar et al. (2015), Liu et al. (2021), and Manga et al. (2017). Furthermore, Nundaeng (2022) conducted a study in which they isolated 41 different yeast species from the rhizosphere of tea plants in Thailand. Among these species, seventeen were identified as *Aureobasidium*, *Galactomyces*, *Kazachstania*, *Saturnispora*, *Schwanomyces*, and *Wickerhamomyces*, while the remaining twenty-four species belonged to *Apiotrichum*,

Curvibasidium, *Papiliotrema*, *Rhodosporidiobolus*, and *Trichosporon*. Nundaeng et al. investigated the effects of *Wickerhamomyces* sp. (SDBR-CMU-S1-06) and *Papiliotremasp.* (SDBR-CMU-S1-02) on the growth of Chinese kale, corn, cucumber, eggplant, lettuce, rice, and tomato plants.

4.7.3 CHNS analysis of compost sets to determine its maturity

Determination of CHNS content in the compost can aid has to determine the C:N ratio which can be utilized to understand the maturity of compost. **Table 9** represents the data of compost for CHNS content which helps to determine the maturity of compost.

Compost sets	Weight (mg)	C%	N%	H%	S%	C/N Ratio
T1	2.737	39.25	3.31	5.329	0.299	11.86
T2	2.352	37.00	3.15	4.722	0.297	11.74
T3	2.133	37.98	3.32	5.059	0.451	11.43
T4	1860	29.09	2.51	4.010	0.196	11.58
T5	1951	29.04	2.35	3.934	0.206	12.35
T6	2085	33.94	2.95	4.447	0.228	11.51

Table 9: Analysis of compost for CHNS content to determine the maturity of compost.

Comparison of Carbon (C),Hydrogen (H), Nitrogen (N) and Sulphur (S) content was done to check in which compost sets the decomposition was faster. **Fig 23** depict the graphical representation of Table 9 data for C, H, N and S content of 25th day compost sets.

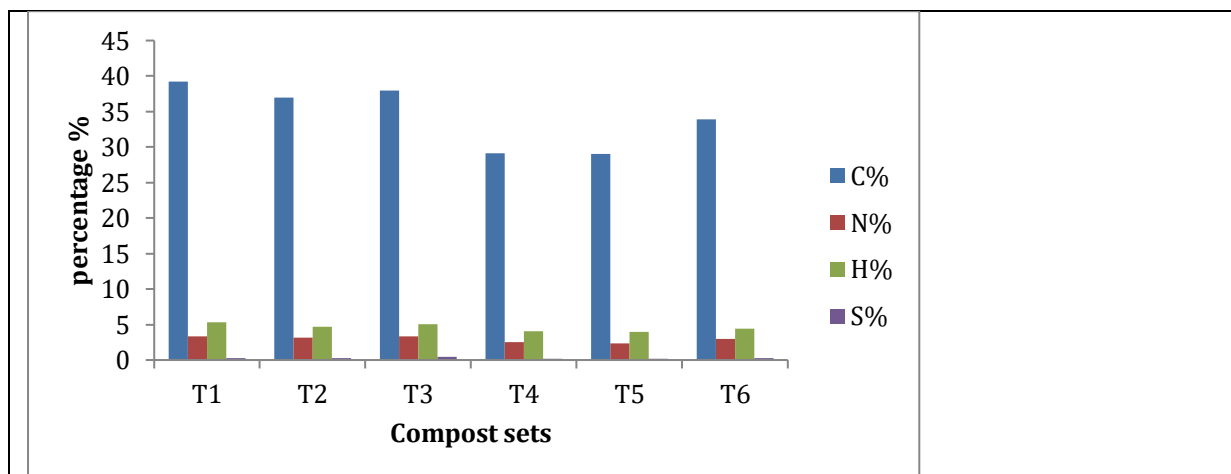


Fig23: CHNS analysis of 25th day compost sets.

A comparison of Carbon:Nitrogen (C:N) ratios was conducted to determine which compost set had reached maturity more rapidly. **Fig 24** depicts the graphical representation of Table 9 data for C:N ratio of 25th day compost sets.

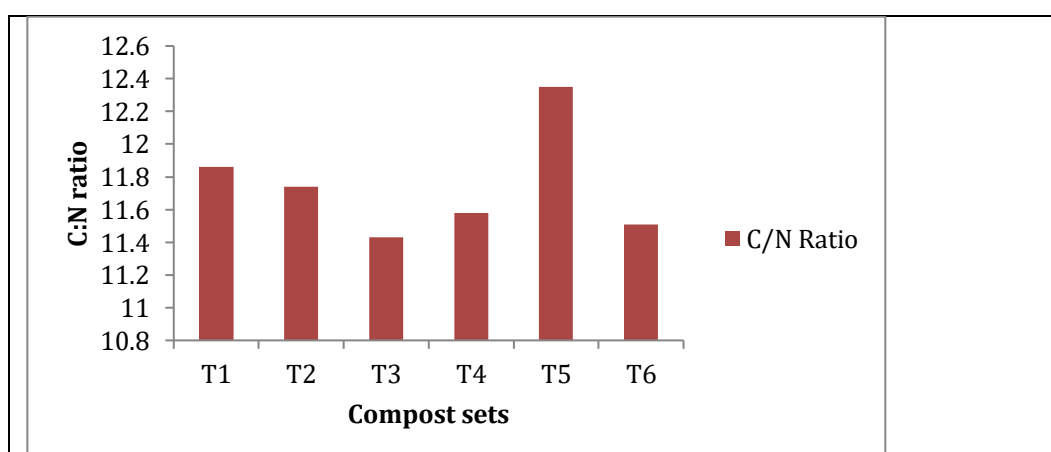


Fig 24: C:N ratio of 25th day compost sets.

As the compost matures, the C:N ratio decreases. The C:N ratio of compost sets T1,T2, T3,T4, T5 and T6 was found to be 11.86, 11.74, 11.43, 11.58, 12.35 and 11.51. All compost

sets showed good compost maturity. Compost T3, in which the culture was added subsequently after 7 days, exhibited the most significant reduction in the C:N ratio, measuring 11.43. This reduction reflects a substantial decrease in total carbon content, suggesting good compost maturity and faster decomposition compared to other compost sets. Also isolate SPDM15 also produces various plant polymer degrading enzymes and survives in extreme conditions.

Studies on municipal green waste by De Bertoldi et al. (1983) revealed that an initial C/N ratio of 25 was optimal, as higher ratios slowed decomposition rates and lower ratios increased nitrogen losses. Tripetchkul et al. (2012) investigated the impact of initial C/N ratios (20, 25, and 30) on C/N ratio evolution during composting. All treatments exhibited a decrease in C/N ratio over time, indicating increasing organic matter humification. The compost piles with initial C/N ratios of 30:1 and 25:1 experienced a more rapid decline in C/N ratio compared to the 20:1 ratio, reflecting faster biodegradation rates and significant organic matter reduction. The initial C/N ratio significantly influenced composting performance, including temperature evolution, organic matter degradation, and total nitrogen loss. Alidadi et al. reported a decline in C/N ratio from 53.57 on the 25th day to 16.6 on the 100th day of composting, primarily attributed to CO₂ emission during the composting process. Similarly, Fourti et al. observed initial C/N ratios of 32 and 28.5 in a two-window system, with net C/N ratios decreasing to 18.6 and 14.6, respectively, by the end of the process. According to many authors, a C/N value below 20 is indicative of acceptable maturity, while a value nearing 12 is often considered a sign of good compost maturity. Morais and Queda (2003) proposed that a ratio below 20 is ideal for achieving compost maturity, with the optimal ratio being less than 15. Nair et al. (2006) achieved a C:N ratio lower than 20 within 21 days by combining thermophilic composting (TC) and vermicomposting (VC). However, in the current study, only those samples inoculated with

Trichoderma sp. and subjected to 21 days of thermophilic composting followed by 7 days of vermicomposting managed to reduce the ratio to below 20.

Conclusion

Based on the experimental results obtained from the analysis of isolate SPDM15, it is evident that salt concentration significantly influenced the growth rate and morphology of the yeast. The absence of salt in the medium resulted in notably low growth rates, with the highest growth observed at a 10% salt concentration, followed by a decrease in growth rate with increasing salinity. Morphological observations revealed distinct changes in yeast structure with varying salt concentrations, ranging from filamentous hyphal structures at 0% salt concentration to bipolar and polar budding at higher salt concentrations. Additionally, the viability of yeast was found to be 1.37×10^9 CFU/ml, indicating robust growth and proliferation after 5 days of incubation in NTYE broth. Pigment extraction from cultures grown in 10% salt medium yielded a black powder pigment, with 28 mg obtained from 50 ml broth. Further characterization via FTIR confirmed the extracted pigment as melanin, demonstrating its insolubility in water and solubility in NaOH and DMSO. Further investigation revealed the enzymatic activities of isolate SPDM15, including amylase, xylanase, pectinase, cellulase, lipase, urease, catalase, esterase, and agarase. However, no detectable levels of laccase and gelatinase enzymes were observed. The yeast isolate also demonstrated positive results for exopolysaccharide (EPS) production. Pathogenicity testing revealed gamma hemolysis on blood agar media, indicative of a lack of hemolysis.

The composting experiment demonstrated efficient organic waste decomposition with optimal moisture content achieved in all sets except for Set 5, requiring additional water maintenance. No foul odour production was noted throughout the experiment. Analysis of volatile solids and ash content revealed varying degrees of biodegradable substances and

inorganic residues among the compost sets, with Set 3 containing the highest biodegradable substances and Set 6 exhibiting the highest inorganic residues. pH levels transitioned from acidic to neutral and eventually alkaline, indicating the progression of composting phases. Temperature monitoring revealed distinct phases of mesophilic, thermophilic, and cooling, crucial for assessing composting progress. Evaluation of compost extract on cowpea seed germination highlighted significant improvements in germination rate and vigor index, with seeds treated with Set 2 extract showing notably higher vigor index compared to the control. These findings indicate the efficacy of composting in organic waste management and its positive impact on seed germination, particularly with specific compost extracts.

The C:N ratio found in all compost sets was below 15, indicating good mature compost. The lowest C:N ratio was in set 3, indicating faster decomposition than the other compost sets in which the culture was subsequently added for 7 days.

The dyeing experiment revealed that cotton fabric treated with mordants such as alum + sodium carbonate and alum + ferrous sulphate showed superior pigment absorption and binding properties, resulting in minimal shade difference even after rigorous washing, wet rubbing, and sunlight exposure. However, natural mordants led to uneven dyeing and subsequent color fading of the fabric after washing and wet rubbing. Mordants including potassium dichromate, ferrous sulphate, and cupric sulphate yielded unsatisfactory dyeing results on cotton fabric. Moreover, antibacterial activity was observed against *Salmonella Typhi*, *Providencia rettgeri*, and *Klebsiella pneumonia* when cotton fabric was dyed with melanin pigment and treated with mordants alum and sodium carbonate, highlighting the potential antimicrobial properties of the dyed fabric. These findings talk about the importance of selecting appropriate mordants to enhance dye absorption and fabric durability, while also considering the potential antimicrobial benefits of certain dyeing processes.

REFERENCES

1. Atlas RM, Parks LC. Handbook of microbiological media. London: CRC Press; 1993.
2. Buzzini P, Martini A. Extracellular enzymatic activity profiles in yeast and yeast-like strains isolated from tropical environments. *J Appl Microbiol.* 2002;93:1020–5.
3. Derguine-Mecheri, L., Kebbouche-Gana, S., Khemili, S., & Djenane, D. (2018). Screening and biosurfactant/bioemulsifier production from a high-salt-tolerant halophilic *Cryptococcus* strain YLF isolated from crude oil. *Journal of Petroleum Science and Engineering*, 162, 712–724. <https://doi.org/10.1016/j.petrol.2017.10.088>
4. Elsayed, A., Mowafy, A. M., Soliman, H. M., Gebreil, A., & Magdy, N. I. (2016). Characterization of new strains of *Hortaea werneckii* isolated from salt marshes of Egypt. *Egyptian Journal of Basic and Applied Sciences*, 3(4), 350–356. <https://doi.org/10.1016/j.ejbas.2016.09.001>
5. Elsayis, A., Hassan, S. W., Ghanem, K. M., & Khairy, H. (2022). Optimization of melanin pigment production from the halotolerant black yeast *hortaea werneckii* AS1 isolated from Solar Salter in Alexandria. *BMC Microbiology*, 22(1). <https://doi.org/10.1186/s12866-022-02505-1>
6. Elsayis, A., Hassan, S. W., Ghanem, K. M., & Khairy, H. (2022b). Suggested Sustainable Medical and Environmental Uses of Melanin Pigment From Halotolerant Black Yeast *Hortaea werneckii* AS1. *Frontiers in Microbiology*, 13. <https://doi.org/10.3389/fmicb.2022.871394>
7. Formoso, A., Heidrich, D., Félix, C. R., Tenório, A. C., Leite, B. R., Pagani, D. M., Ortiz-Monsalve, S., Ramírez-Castrillón, M., Landell, M. F., Scroferneker, M. L., & Valente, P. (2015). Enzymatic Activity and Susceptibility to Antifungal Agents of

- Brazilian Environmental Isolates of *Hortaea werneckii*. *Mycopathologia*, 180(5–6), 345–352. <https://doi.org/10.1007/s11046-015-9920-3>
8. Gorjan, A., & Plemenitaš, A. (2006). Identification and characterization of ENA ATPases Hwena1 and HWENA2 from the halophilic black yeast *hortaea werneckii*. *FEMS Microbiology Letters*, 265(1), 41–50. <https://doi.org/10.1111/j.1574-6968.2006.00473.x>
 9. Gunde-Cimerman, N., & Plemenitaš, A. (2006). Ecology and molecular adaptations of the halophilic black yeast *Hortaea werneckii*. *Reviews in Environmental Science and Bio/Technology*, 5(2–3), 323–331. <https://doi.org/10.1007/s11157-006-9105-0>
 10. Gunde-Cimerman, N., Ramos, J., & Plemenitaš, A. (2009). Halotolerant and halophilic fungi. *Mycological Research*, 113(11), 1231–1241. <https://doi.org/10.1016/j.mycres.2009.09.002>
 11. Gientka, I., Błażej, S., Stasiak-Róžańska, L., & Chlebowska-Śmigiel, A. (2015). Exopolysaccharides from yeast: insight into optimal conditions for biosynthesis, chemical composition and functional properties – review. *Acta Scientiarum Polonorum*, 14(4), 283–292. <https://doi.org/10.17306/j.afs.2015.4.29>
 12. Helan, M. H. M., Rani, S., Ramesh, T., Subramanian, J., & Kalaiselvam, M. (2013). Production and Characterization of Melanin Pigment from Halophilic Black Yeast *Hortaea werneckii*. *International Journal of Pharma Research & Review*. <https://www.rroj.com/open-access/production-and-characterization-of-melanin-pigment-from-halophilic-black-yeast-hortaea-werneckii.pdf>
 13. Hodhod, M. S., Gaafar, A. Z., Alshameri, A., Qahtan, A. A., Noor, A., & Abdelwahab, M. A. (2020). Molecular characterization and bioactive potential of newly identified strains of the extremophilic black yeast *Hortaea werneckii* isolated

- from Red Sea mangrove. *Biotechnology & Biotechnological Equipment*, 34(1), 1288–1298. <https://doi.org/10.1080/13102818.2020.1835535>
14. Jouhara, H., Czajczyńska, D., Ghazal, H., Krzyżyńska, R., Anguilano, L., Reynolds, A., & Spencer, N. (2017). Municipal waste management systems for domestic use. *Energy*, 139, 485–506. <https://doi.org/10.1016/j.energy.2017.07.162>
15. Kejžar, A., Gobec, S., Plemenitaš, A., & Lenassi, M. (2013). Melanin is crucial for growth of the black yeast *Hortaea werneckii* in its natural hypersaline environment. *Fungal Biology*, 117(5), 368–379. <https://doi.org/10.1016/j.funbio.2013.03.006>
16. Kogej, T., Stein, M., Volkmann, M., Gorbushina, A. A., Galinski, E. A., & Gunde-Cimerman, N. (2007b). Osmotic adaptation of the halophilic fungus *Hortaea werneckii*: role of osmolytes and melanization. *Microbiology*, 153(12), 4261–4273. <https://doi.org/10.1099/mic.0.2007/010751-0>
17. Leitgeb, M., Čolnik, M., Primožič, M., Zalar, P., Cimerman, N. G., & Knez, Ž. (2013). Activity of cellulase and α -amylase from *hortaea werneckii* after cell treatment with supercritical carbon dioxide. *The Journal of Supercritical Fluids*, 78, 143–148. <https://doi.org/10.1016/j.supflu.2013.03.029>
18. Mahapatra, S., Ali, M. H., & Samal, K. (2022). Assessment of compost maturity-stability indices and recent development of composting bin. *Energy Nexus*, 6, 100062. <https://doi.org/10.1016/j.nexus.2022.100062>
19. Petrovič, U., Gunde-Cimerman, N., & Plemenitaš, A. (1999). Salt stress affects sterol biosynthesis in the halophilic black yeast *Hortaea werneckii*. *FEMS Microbiology Letters*, 180(2), 325–330. <https://doi.org/10.1111/j.1574-6968.1999.tb08813.x>
20. Plemenitaš, A., & Gunde-Cimerman, N. (2005). Cellular responses in the halophilic black yeast *hortaea werneckii* to high environmental salinity. In *Springer eBooks* (pp. 453–470). https://doi.org/10.1007/1-4020-3633-7_29

21. Plemenitaš, A., Vaupotič, T., Lenassi, M., Kogej, T., & Gunde-Cimerman, N. (2008b). Adaptation of extremely halotolerant black yeast *Hortaea werneckii* to increased osmolarity: a molecular perspective at a glance. *Studies in Mycology*, *61*, 67–75. <https://doi.org/10.3114/sim.2008.61.06>
22. Rizk, S. M., & Magdy, M. (2022). An indigenous inland genotype of the black yeast *Hortaea werneckii* inhabiting the great pyramid of Giza, Egypt. *Frontiers in Microbiology*, *13*. <https://doi.org/10.3389/fmicb.2022.997495>
23. Samal, K., Dash, R. R., & Bhunia, P. (2018). Effect of hydraulic loading rate and pollutants degradation kinetics in two stage hybrid macrophyte assisted vermifiltration system. *Biochemical Engineering Journal*, *132*, 47–59. <https://doi.org/10.1016/j.bej.2018.01.002>
24. Stephen, D. W., & Jamieson, D. J. (1996). Glutathione is an important antioxidant molecule in the yeast *Saccharomyces cerevisiae*. *FEMS Microbiology Letters*, *141*(2–3), 207–212. <https://doi.org/10.1111/j.1574-6968.1996.tb08386.x>
25. Śliżewska, W.; Struszczyk-Świta, K.; Marchut-Mikołajczyk, O. Metabolic Potential of Halophilic Filamentous Fungi—Current Perspective. *Int. J. Mol. Sci.* *2022*, *23*, 4189. <https://doi.org/10.3390/ijms23084189>
26. Śliżewska, W., Struszczyk-Świta, K., & Marchut-Mikołajczyk, O. (2022). Metabolic Potential of Halophilic Filamentous Fungi—Current Perspective. *International Journal of Molecular Sciences*, *23*(8), 4189. <https://doi.org/10.3390/ijms23084189>
27. Tang, J., Kanamori, T., Inoue, Y., Yasuta, T., Yoshida, S., & Katayama, A. (2004). Changes in the microbial community structure during thermophilic composting of manure as detected by the quinone profile method. *Process Biochemistry*, *39*(12), 1999–2006. <https://doi.org/10.1016/j.procbio.2003.09.029>

28. Thomas P, Sekhar AC, Upreti R, Mujawar MM, Pasha SS. Optimization of single plate-serial dilution spotting (SP-SDS) with sample anchoring as an assured method for bacterial and yeast cfu enumeration and single colony isolation from diverse samples. *Biotechnol Rep (Amst)*. 2015 Aug 20;8:45-55. doi: 10.1016/j.btre.2015.08.003. PMID: 28352572; PMCID: PMC4980700.
29. Uhm C, Jeong H, Lee SH, Hwang JS, Lim KM, Nam KT. Comparison of structural characteristics and molecular markers of rabbit skin, pig skin, and reconstructed human epidermis for an ex vivo human skin model. *Toxicol Res*. 2023 May 4;39(3):477-484. doi: 10.1007/s43188-023-00185-1. PMID: 37398575; PMCID: PMC10313609.
30. Zalar, P., Zupančič, J., Gostinčar, C., Zajc, J., De Hoog, G., De Leo, F., Azúa-Bustos, A., & Gunde-Cimerman, N. (2019). The extremely halotolerant black yeast *Hortaea werneckii* - a model for intraspecific hybridization in clonal fungi. *IMA Fungus*, 10(1). <https://doi.org/10.1186/s43008-019-0007-5>

APPENDIX I :MEDIA COMPOSITION**NaCl Tryptone Yeast Extract Broth**

Ingredients	g/l
NaCl/crude salt	0,50,10,150,200,250,300
MgSO ₄ .7H ₂ O	20
KCl	5
Tryptone	5
Yeast extract	3
Final pH	7.1 ± 0.2

NaCl Tryptone Yeast Extract Agar

Ingredients	g/l
NaCl/crude salt	0,50,10,150,200,250,300
MgSO ₄ .7H ₂ O	20
KCl	5
Tryptone	5
Yeast extract	3
Agar	20
Final pH	7.1 ± 0.2

Congo red agar

Ingredients	g/l
Brain heart infusion broth	37
Sucrose	50
Agar	20
Congo red stain	0.8
Final pH	7.1 ± 0.2

CTAB methylene blue agar

Ingredients	g/l
Cetyltrimethylammonium bromide	0.2
Methylene blue	0.005
MgSO ₄ .7H ₂ O	20
KCl	5
Tryptone	5
Yeast extract	3
Agar	20
Final pH	7.1 ± 0.2

Starch NTYE agar

Ingredients	g/l
NaCl/crude salt	100
Soluble starch	20
MgSO ₄ .7H ₂ O	20
KCl	5
Tryptone	5
Yeast extract	3
Agar	20
Final pH	7.1 ± 0.2

CMC NTYE agar

Ingredients	g/l
Carboxymethyl Cellulose	20
Nacl/crude salt	100
MgSO ₄ .7H ₂ O	20
KCl	5
Tryptone	5
Yeast extract	3
Agar	2%
Final pH	7.1 ± 0.2

Skimmed milk NTYE agar

Ingredients	g/l
Skimmed milk	20
MgSO ₄ .7H ₂ O	20
KCl	5
Tryptone	5
Yeast extract	3
Agar	2%
Final pH	7.1 ± 0.2

Mueller Hinton agar

Ingredients	g/l
Beef Extract	2
Acid Hydrolysate of Casein	17.50
Starch	1.50
agar	20
Final pH	7.1 ± 0.2

Tributylin NTYE agar

Ingredients	g/l
tributylin	20
MgSO ₄ .7H ₂ O	20
KCl	5
Tryptone	5
Yeast extract	3
Agar	20
Final pH	7.1 ± 0.2

Tween 80 NTYE agar

Ingredients	g/l
Tween 80	10
NaCl/crude salt	100
MgSO ₄ .7H ₂ O	20
KCl	5
Tryptone	5
Yeast extract	3
Agar	2%
Final pH	7.1 ± 0.2

Blood agar

Ingredients	g/l
Peptone	5
Beef extract	3
NaCl	5
Agar	20
Final pH	7.1 ± 0.2

Pectin NTYE agar

Ingredients	g/l
Pectin	20
NaCl/crude salt	100
MgSO ₄ .7H ₂ O	20
KCl	5
Tryptone	5
Yeast extract	3
Agar	2%
Final pH	7.1 ± 0.2

Gelatin NTYE broth

Ingredients	g/l
Gelatin	20
NaCl/crude salt	100
MgSO ₄ .7H ₂ O	20
KCl	5
Tryptone	5
Yeast extract	3
Final pH	7.1 ± 0.2

Urea NTYE agar

Ingredients	g/l
Urea	20
Nacl/crude salt	100
MgSO ₄ .7H ₂ O	20
KCl	5
Tryptone	5
Yeast extract	3
Phenol red	0.012
Agar	2%
Final pH	7.1 ± 0.2

Sea water NTYE agar

Ingredients	g/l
MgSO ₄ .7H ₂ O	20
KCl	5
Tryptone	5
Yeast extract	3
Sea water	1000 L
Agar	2%
Final pH	7.1 ± 0.2

ABTS NTYE agar

Ingredients	g/l
ABTS	0.1
MgSO ₄ .7H ₂ O	20
KCl	5
Tryptone	5
Yeast extract	3
Agar	20
Final pH	7.1 ± 0.2

Xylan agar

Ingredients	g/l
Xylan	20
NaCl/crude salt	100
MgSO ₄ .7H ₂ O	20
KCl	5
Tryptone	5
Yeast extract	3
Agar	20
Final pH	7.1 ± 0.2

APPENDIX II: REAGENT**Chloramphenicol**

Chloramphenicol	0.25g
95% ethanol	10 ml

Ethanol

Ethanol (ml)	Distilled water (ml)	Percentage (%)
10	90	10
30	70	30
50	50	50
70	30	70
90	10	90
100	0	100

Glutaraldehyde solution

Glutaraldehyde	2.5g
Distilled water	100ml

Iodine solution

Iodine	0.2g
KI	0.4g
Distilled water	100ml

0.1% Congo red

Congo red	0.1g
Distilled water	100ml

Lugol's Iodine solution

Iodine	1.0g
Potassium iodide	2.0g
Distilled water	300ml

3% Hydrogen peroxide

Hydrogen peroxide	3ml
Distilled water	97ml

2% of Sodium hypochlorite

Sodium hypochlorite	2ml
Distilled water	98ml

1N NaOH

NaOH	4g
Distilled water	100ml

10mg/ml Melanin

Melanin	0.01g
DMSO	1ml

1M HCl

HCl	3.65
Distilled water	96.35

5% Alum

Alum	5g
Distilled water	100ml

